

GENERATION OF MATLAB SOFTWARE TOOL FOR TEACHING STEM CONCEPTS
USING GREENPOWER FORMULA 24 RACE CARS

By

Andrew Scott Rivers

Raga Ahmed
Associate Professor of Engineering
(Chair)

Vahid R. Disfani
Assistant Professor of Engineering
(Committee Member)

Nurhidajat Sisworahardjo
Associate Professor of Engineering
(Committee Member)

GENERATION OF MATLAB SOFTWARE FOR TEACHING STEM CONCEPTS USING
GREENPOWER FORMULA 24 RACE CARS

By

Andrew Scott Rivers

A Thesis Submitted to the Faculty of the University of
Tennessee at Chattanooga in Partial
Fulfillment of the Requirements of the Degree
of Master of Science: Engineering

The University of Tennessee at Chattanooga
Chattanooga, Tennessee

December 2022

Copyright © 2022

By Andrew Scott Rivers

All Rights Reserved

ACKNOWLEDGMENTS

I would like to thank my committee chair, Dr. Raga Ahmed, and my committee members, Dr. Nurhidajat Sisworahardjo, and Dr. Vahid R. Disfani, for their guidance and support throughout the course of this research.

In addition, I would also like to thank my friends, colleagues, the department faculty, and staff for making my time at The University of Tennessee at Chattanooga a wonderful experience.

ABSTRACT

Greenpower Formula 24 races are a prime opportunity for STEM educators to engage young students in STEM activities and increase their interest and content knowledge in the STEM fields. MATLAB AppDesigner is utilized to construct a graphical user interface (GUI) for the purpose of simulating the performance of Greenpower's Formula 24 electric race cars. This menu driven interface allows students to manipulate design variables and observe the effect on performance indicators. Hardware bench testing and finite element analysis software were utilized to determine, respectively, parameters for modeling the electric car's drive-train components and for modeling aerodynamic components. This GUI is intended to be offered to all Greenpower USA teams who compete in a Formula 24 category. The expected impact is to increase the competitiveness, confidence, and competence of race participants, and more broadly to aid STEM project-based teaching and learning.

TABLE OF CONTENTS

ACKNOWLEDGMENTS	iv
ABSTRACT	v
LIST OF FIGURES	viii
LIST OF TABLES.....	x
CHAPTER I.....	1
1.1 Motorsports in Promoting STEM Education	1
1.2 Greenpower Competition: History and Untapped Potential	3
1.3 Literature Review and the Void to Fill	4
1.4 Objectives.....	5
1.5 Outline of Thesis	6
CHAPTER II	7
2.1 Greenpower Formula 24 Race Description.....	7
2.2 Greenpower Formula 24 Categories	7
2.3 Commonalities Between Categories	9
2.4 Race Day	9
2.5 Problem Statement	10
CHAPTER III	12
3.1 Overview.....	12
3.2 Modeling and Derivation of GUI Outputs	17
3.2.1 Wheels and Tires.....	17
3.2.2 Motors	24
3.2.3 Gearing.....	28
3.2.4 Motor Control	28
3.2.5 Battery	29
3.2.6 Aerodynamics	35
3.2.7 Force and Power.....	40
3.2.8 Output Plots.....	42
3.2.9 Numeric Output Fields.....	45
3.2.10 Help Functions	48
CHAPTER IV	50
4.1 Machine Ratings	50

4.2 Motor Armature Resistance	51
4.3 Motor Armature Inductance.....	53
4.4 Swinburn Tests.....	55
4.5 Determining No-Load Speed, Torque-Speed Characteristics and Motor Regulation	60
4.7 Steady State Motor Temperature	69
CHAPTER V	76
5.1 Conclusion	76
5.2 Future Work	77
REFERENCES.....	79
VITA.....	81

LIST OF FIGURES

Figure 1 Stock Class Frame as Modeled in Siemens SolidEdge	8
Figure 2 Main Program Window with Help Buttons Marked as '?'	13
Figure 3 Crr Dependence on Innertube.....	19
Figure 4 ΔCrr Dependence on Innertube	20
Figure 5 Schwalbe Kojak Crr VS Tire Pressure	22
Figure 6 Schwalbe Durano Crr VS Tire Pressure	23
Figure 7 Comparison of Crr for the Schwalbe Kojak and Durano Versus Tire Pressure.....	24
Figure 8 FRACMO Motor Characteristic Curves.....	25
Figure 9 Shanbo EM Motor Characteristic Curves.....	26
Figure 10 Yuasa Battery Specifications.....	30
Figure 11 Yuasa Discharge Characteristics	31
Figure 12 AJC-D35S Battery Specifications	32
Figure 13 AJC-D35S Discharge Characteristics.....	33
Figure 14 Battery Voltage VS State of Charge.....	35
Figure 15 Simplified CAD Model $\frac{3}{4}$ View.....	36
Figure 16 Simplified CAD Model Front View	37
Figure 17 Boundary Cartesian Box Dimensions	39
Figure 18 CFD Mesh Settings.....	39
Figure 19 Cross Section of Mesh Depicting Refinements.....	40

Figure 20 Power Consumption of the Car	43
Figure 21 Characteristic Curves of the Shanbo Greenpower Motor.....	44
Figure 22 Overlay of Required Power, Motor Power and Motor Efficiency	45
Figure 23 Help Dialogue.....	49
Figure 24 Schematic for Inductance Measurement [24].....	54
Figure 25 FRACMO Constant Power Loss VS Speed	56
Figure 26 Motion Tech Constant Power Loss VS Speed	56
Figure 27 Shanbo EM Constant Power Loss VS Speed	57
Figure 28 FRACMO Efficiency Versus Speed.....	58
Figure 29 Motion Tech Efficiency Versus Speed.....	59
Figure 30 Shanbo EM Efficiency Versus Speed.....	59
Figure 31 Shanbo EM Motor Coupled to the Motorsolver Generator.....	61
Figure 32 FRACMO Current Versus Speed	63
Figure 33 Motion Tech Current Versus Speed	64
Figure 34 Shanbo EM Current Versus Speed.....	64
Figure 35 FRACMO Torque-Speed Curve.....	67
Figure 36 Motion Tech Torque-Speed Curve.....	67
Figure 37 Shanbo EM Torque-Speed Curve.....	68
Figure 38 Motor Temperature Setup.....	70
Figure 39 Motor Controller and Connections.....	71
Figure 40 DEScribe Custom Test Setup	72
Figure 41 Motor Temperature Versus Time	74

LIST OF TABLES

Table 1 Summary of GUI Components and Functions Covered	14
Table 2 Summary of Rolling Resistance Versus Tire Pressure for Different Innertubes	19
Table 3 Difference in Crr Based on Innertube and Pressure	20
Table 4 Percent Difference in Crr Based on Innertube and Pressure	21
Table 5 Schwalbe Kojak <i>Crr</i> Versus Tire Pressure	21
Table 6 Schwalbe Durano <i>Crr</i> Versus Tire Pressure	22
Table 7 Common Data Points for the Schwalbe Kojak and Durano	23
Table 8 Comparison of Battery Capacity Ratings and Internal Resistance	33
Table 9 Peukert Constants of the AJC and Yuasa Batteries	34
Table 10 Greenpower Motor Nameplate Ratings	50
Table 11 Motor Solver Generator Nameplate Ratings	51
Table 12 FRACMO Armature Resistance	52
Table 13 Motion Tech Armature Resistance	52
Table 14 Shanbo EM Armature Resistance	53
Table 15 Summary of Armature Inductances	55
Table 16 Summary of Motor Efficiencies	60
Table 17 Summary of No-Load Currents	60
Table 18 Encoder Frequency Output and Motor Current Draw	61
Table 19 Motor Speed Under Open Circuit Generator Load.....	62

Table 20 Stall Current of Each Motor.....	62
Table 21 Ordered Pairs of Current and Speed	63
Table 22 Summary of Ideal No-Load Motor Speeds.....	65
Table 23 Summary of Actual No-Load Motor Speeds and Currents.....	65
Table 24 Motor Speed Constants	66
Table 25 Motor Torque Constants	66
Table 26 Summary of Motor Regulation	68
Table 27 Motor Controller Ratings.....	69
Table 28 Motor Temperature Change Per Unit Time.....	74

CHAPTER I

INTRODUCTION

1.1 Motorsports in Promoting STEM Education

Educators and policy makers have increasingly been focusing on promoting student persistence and success in STEM (Science, Technology, Engineering and Math) learning and on preparing students for careers in the STEM fields [1]. This thesis presents a tool for STEM education that promotes exploring STEM concepts in the context of the popular and interesting Greenpower car race competition. By harnessing the positive impact of stimulating interest which improves focus and bolsters learning outcome, this work aims to increase student engagement in learning and to facilitate teacher or mentor implementation of student-directed project-based learning. It has been suggested in [1] that situational interest (interest stimulation by a learning environment such as a competition) is often a gateway to developing interest in a specific domain (such as math) and vice versa. The authors point out that people's interests motivate them to pay attention to material that they find appealing and in so doing they experience a positive affect that further reinforces their interest and cognitive effort, people attend selectively to content in their environment that is consistent with their interests. Motorsports represent one of the most interest-generating and exciting activities for students and have been promoted as effective learning tools with demonstrable interest by secondary school students at the stage of pursuing college enrollment [2]. Indiana University Purdue University

Indianapolis (IUPUI), which was the first in the United States to offer a Bachelor of Science Degree in Motorsports Engineering, has recognized motorsports as an excellent mechanism to promote STEM education since it is attractive to students regardless of demographics. IUPUI has developed, implemented, and promoted a summer program focused on motorsports and has recommended that STEM educators should consider integrating motorsports activities in their classroom guided by teaching modules disseminated locally to schools [2]. More details about the author's involvement can be found in [3]. A 6-week intensive pre-college summer STEM program has been implemented at the Cooper Union for the Advancement of Science and Art with focus on the SAE International competition; high school students, mentored by college students, choose a motorsports project of most interest to them and engage in design, analysis, testing and documentation this effort is claimed to increase student retention in STEM [4]. Students in Utah that participate in a Greenpower Electric Car Challenge are given access to relevant online lessons developed by a professor at Utah State University. The challenge, which targets energy efficiency and fast performance, is sponsored by Utah Governor's Office of Energy through an investment with the Energy Department's State Energy Program [5]. As mentioned at the beginning of this chapter, this work focuses on the Greenpower car races. Description of this race is found in Chapter 2. The following section provides a historical prospective on the race and highlights opportunities to contribute to increasing participants.

1.2 Greenpower Competition: History and Untapped Potential

In 1999, the Greenpower Education Trust began as a way of introducing school aged children to science, technology, engineering, and math (STEM) in the UK [6]. The goal of the Education Trust is to organize a competition for students to design, build and race small electric cars in an endurance event with the aim of rewarding energy efficiency. Teams aim to maximize the distance travelled in a given time period in an electric vehicle they design while observing given rules. Since 1999, Greenpower has spread to the United States, South Africa, Poland, and China, all with the same goal of promoting STEM activities [6]. Though the majority of the design engineering has been completed by the governing body to ensure safe and fair competition, the rules permit numerous areas of design, including aerodynamics, thermodynamics, and electromechanical systems, to be explored. The Greenpower rules dictate that the students must make their own design decisions for the car so long as they are within the scope of the rules. Each team has an adult mentor or mentors with whom they may consult, but the mentor(s) may not make any design decisions themselves. This minimal involvement of school faculty promotes the student's critical thinking and reasoning skills while maintaining order and safety. The mentors are generally faculty at the school which the students attend, or a parent of a student involved with Greenpower. Though an effective method of ensuring the mentors are interested in the competition, this approach leads to inconsistencies in their backgrounds and therefore also a discrepancy in their ability to answer the students' technical/engineering questions. Without a consistent in-team source of expertise, each team is left to find outside means of answering the technical/engineering questions for the competition. This causes some teams to be better equipped than others for the design of their cars.

With differences in sponsorship, support, and finances between the teams, there is currently a large variation in design approaches, often simply based on best practices as viewed by the team. Though this leads to a diverse grid, it also widens the gap between the wealthier, better supported teams and those with less.

1.3 Literature Review and the Void to Fill

The previous sections provided a survey of the literature on motorsports in general and Greenpower competition in particular in STEM education. It can be seen that there is a void to fill in the literature; in particular, there is a lack of software tools available to the Greenpower USA teams, mentors, teachers, and students to guide efficient operation of their race car. Instead, expensive empirical testing is relied upon along with small amounts of data acquisition to determine changes which should be made to the car to improve efficiency. Many teams lack the budget to test all their ideas for their Formula 24 category cars. This results in long delays in taking a concept to fruition. Software tools available to all teams are presently limited to Siemens Solid Edge for Computer Aided Design (CAD) and spreadsheets for data evaluation. This limited set of tools does not permit an in-depth discussion to be had not only within the teams, but among them as well. It is possible for a team to develop their own software for use in the competition, but development of such tools is costly, both financially and in terms of time. A dedicated software tool available to all involved in Greenpower, would help level and increase the competition. There has been one well-documented attempt to solve this issue. The Rotary Racer Greenpower UK team at Chipping Sodbury developed a web browser-based simulation tool similar to the one presented in [8]. It has, however, not been updated in several years at the time of this writing. Rule changes, component availability and technology improvements have all

resulted in this tool being outdated. It is therefore the goal of this thesis to develop and present a MATLAB based GUI with the intent to allow teams involved in the Formula 24 categories to simulate changes to their vehicles without the cost and time associated with empirical tests. In this work, mechanical parameters needed for the simulation underlying models are determined via finite element analysis and experimental testing, electrical parameters via hardware bench testing. Access to and use of the GUI would encourage the students to ask more in-depth questions about the STEM topics involved in the design and construction of their cars. The menu driven nature of the tool allows visualization of all the independent variables at once while also providing numerical and graphical feedback on the state of the car's performance. This feedback includes quantities such as the approximate range of the vehicle, the point on the motor efficiency curve where the car is operating under steady state, and the maximum speed of the car. Though many of the concepts presented in the framework are complex, students can learn at an age-appropriate level through selective use of features.

1.4 Objectives

The main objective of this work is to equip mentors, teachers and students with a tool and a software framework that will help them increase student's content knowledge, confidence, and competence. The software developed herein is intended to be available to Formula 24 teams and the schools hosting teams.

1.5 Outline of Thesis

The structure of this work is as follows: Chapter 2 reviews the problem space and the present state of competition in Greenpower USA sanctioned events. The third chapter provides an in depth look into the vehicle components and how the models for them were developed. Experimental testing will be discussed in Chapter 4 along with the methods used and their ties to the GUI. The fifth and final chapter concludes this work and provides suggestions for future work.

CHAPTER II

PROBLEM STATEMENT AND CONTEXT

2.1 Greenpower Formula 24 Race Description

Greenpower races are competitive all-day races targeting mainly middle school and high school students. The goal is to design and build an electric car and to drive it the longest distance in 90 minutes on one battery charge (regenerative braking is allowed). The following sections describe competing categories and what happens on race day.

2.2 Greenpower Formula 24 Categories

Greenpower Formula 24 cars, in the category named *stock* class, are small square tube-steel-framed vehicles which use bicycle wheels 20" in diameter. The cars are one-wheel drive with a direct chain reduction from the motor to the left rear wheel. All necessary mechanical and electrical components are provided in kit form and are forbidden to be altered. Only three tires are approved for use in this class, tire pressures are also limited to 65 psi [7]. The speed of the cars is controlled by the driver via a button on the steering wheel. This button actuates a contactor, directly connecting the batteries to the motor.

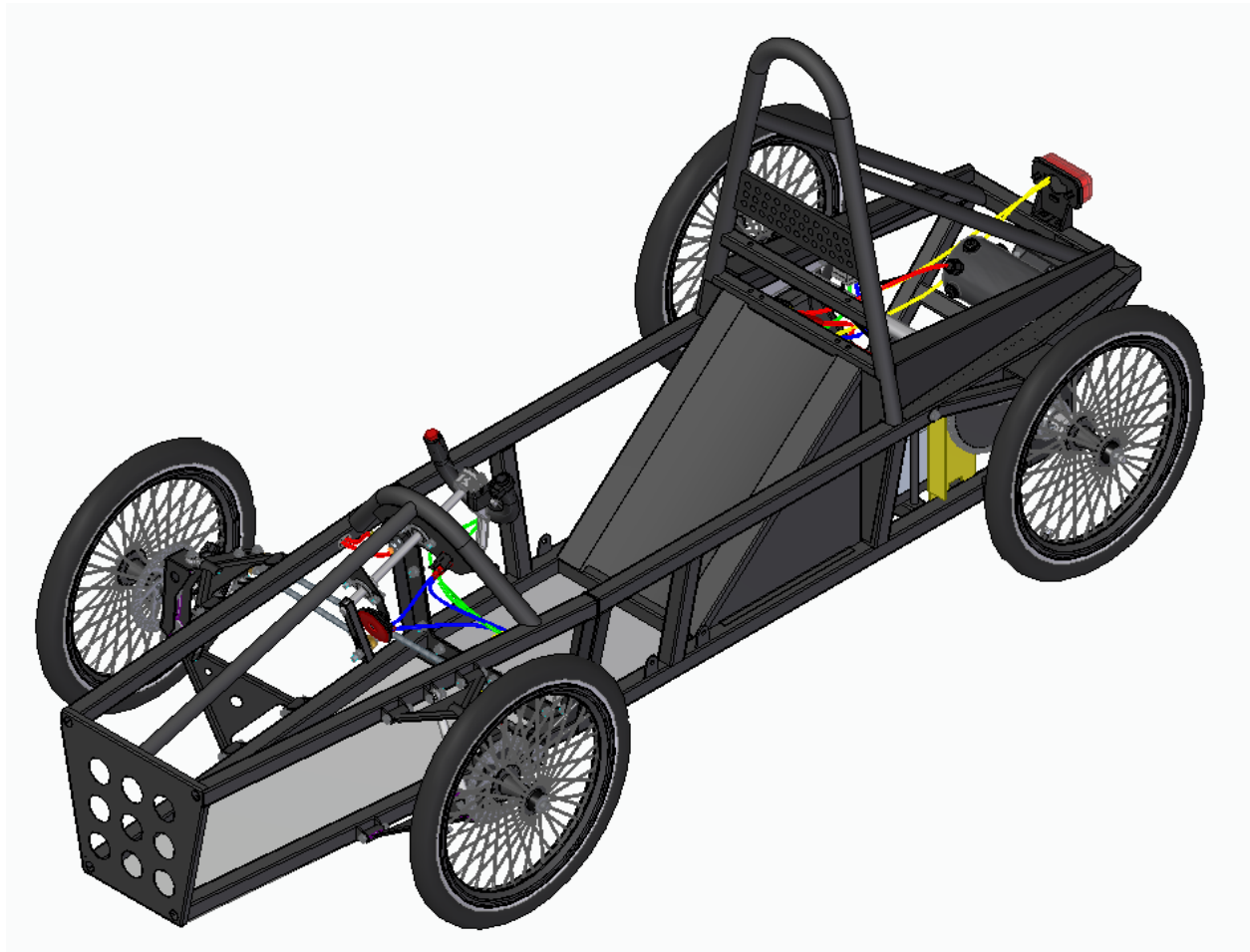


Figure 1 Stock Class Frame as Modeled in Siemens SolidEdge

The ***Modified*** category allows the stock chassis and electrical components to be changed. Teams in this class may choose to make modifications such as use different sprocket tooth counts, add a motor controller, or change the wheel diameter and tire choice, or simply increase the tire pressures.

The *Custom* class of Formula 24 Cars allows the most deviation from the stock chassis. It may be based on the frame provided in the Stock class kit, or entirely designed and built from scratch. Motor controllers are common in this level of competition as are significantly more aerodynamic body designs than the previous two classes.

2.3 Commonalities Between Categories

In all three categories described above, the motors and batteries are a constant. All use the same, or equivalent, 24V brushed DC motors, which may not be opened or modified in any way. There is a choice of two different battery manufactures, Interstate and Yuasa. Deemed equivalent by the rules, the only two model numbers of battery permissible in any of the classifications are the Interstate DCM0035 and the Yuasa REC36-12. Both batteries are 12V Absorbent Glass Mat (AGM) Lead Acid.

2.4 Race Day

During a Formula 24 event, there are several smaller events which take place. The two main events are namely a presentation by the teams to a panel of judges about the cars they have designed and constructed as well as a 90-minute endurance race. The tracks on which the races are held are often set up in large parking lots with cones and small barriers, though some schools have dedicated circuits to host events. The tracks are typically less than one mile in length and relatively simple in layout. Though different categories may be on track at the same time during the race, they are only scored against cars of like classification. The goal of each race is to travel as far as possible on a single battery charge during the race duration. If a car is unable to complete the race, it is either retired or entered into “exhibition” mode where it is allowed to

continue to participate but is not ranked in points [7]. As would be expected, the more improvements made to the cars from the stock chassis, the greater a distance they tend to travel. Pit stops and driver changes are mandatory in all classes. A minimum of two driver changes are required during a 90-minute race and each driver must spend at least 15-minutes in the car [7]. At the Toyota Classic in Huntsville Alabama on relatively level ground during the 2021 season, the winning Stock class car completed 66 laps around a 0.5-mile circuit, while the winning Modified class car completed 70 laps. Though this is only an average speed of approximately 22 mph for the stock class car, it is equivalent to 18.55 Wh/mi, making the Greenpower car over 10 times as efficient as a typical electric road car [8]. Estimating the energy density of E10 gasoline to be 34020 Wh/Gal, this is 1834 MPGe or approximately 76 times as efficient as the average gasoline powered car in the US [9].

2.5 Problem Statement

Promotion and support of STEM education remains an important and motivated goal. Greenpower's Formula 24 competitive electric car race is a popular, interest-generating competition with a lot of potential remaining to be harnessed towards this goal. In this thesis, a software tool for promoting STEM education in the context of Greenpower Formula 24 races is developed. The tool implementation from a user viewpoint is centered on a graphical user interface to be used in simulating the performance of Greenpower's Formula 24 electric race cars. This menu driven interface allows students to manipulate design variables and observe the effect on performance indicators. Several tasks were needed to build functionality into the GUI and populate the built-in help content:

- Computation of performance

Hardware bench testing

Finite element analysis

In order to compute motor performance, it was necessary to understand the armature resistance, constant power losses, no load speed and steady state operating temperature.

Hardware bench testing was utilized to develop accurate models of each of the major components of the cars wherever possible. Finite element analysis was utilized to develop an understanding of the aerodynamic drag of the cars and the same CAD model was used to calculate the frontal area of the vehicle.

By making this tool available to race participants, the aim is to bolster student engagement in learning of concepts and skills and acquisition of content knowledge and to facilitate teacher or mentor implementation of student-directed project-based learning.

CHAPTER III

GRAPHICAL USER INTERFACE DESCRIPTION

3.1 Overview

As stated in the previous chapter, a MATLAB application was constructed in the Appdesigner environment as it provides an efficient method of developing a GUI. As the partial intent of this work is to develop a learning and teaching tool, having an intuitive GUI is pivotal. Figure 2 depicts the main program window when the application is run. This chapter provides an overview of the application, its functionality, and derivations of its models.

Simulation Control

Speed & Power

Drive Sprocket: 12 ?

Driven Sprocket: 72 ?

Drive Ratio: 1: 6 ?

Max Speed (MPH): 23.2 ?

Required Motor Output (W): 286.7 ?

Required Torque (Nm): 1.17 ?

Range @ Speed (mi): 34.95 ?

Acceleration Energy (Wh): 57.99 ?

0 - Max Speed Time (s): 28.34 ?

Motor Regulation (RPM/Nm): 162.9 ?

Resistance Dominance: Rolling resistance dominates air drag ?

Physical Dimensions

Select Body Style: Basic F24 Body ?

Ride Height (mm): 30 ?

Cd: 0.58 ?

A (m²): 0.35 ?

CdA (m²): 0.203 ?

Total Mass (Kg): 145 ?

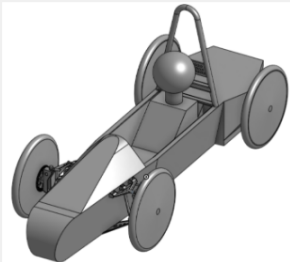
Wheel Dia.": 20 ?

Tire Selection: Schwalbe Kojak ?

Tire Pressure (PSI): 40 ?

Tube Type: Butyl Tube ?

Bearings: Standard ?



Parameter Input/Output

Load Parameters ?

Save Parameters ?

Browse to File ?

Optimization

Target Cruising Speed: 0 ?

Set CVX Path ?

Optimize Gear Ratio ?

Optimize Target Cruising Speed ?

Optimized Cruising Speed: 0 ?

Battery

Battery: Yuasa REC36-12 ?

Series Connected Batteries: 2 ?

Parallel Connected Batteries: 1 ?

Min Batt Voltage: 10.8 ?

Low Voltage Warning: ?

Current Draw (A): 13.82 ?

C Rate: 0.384 ?

Wh Available: 553.2 ?

Discharge Time (MIN): 95.87 ?

Safety Factor: 1.065 ?

Battery Side Power (W): 349.7 ?

Battery Side Voltage: 25.21 ?

Battery SOC: 100 ?

Simulate Full Discharge Cycle ?

Race & Track Conditions

Elevation Change: Low ?

Custom Elevation Change (m): 0 ?

Race Duration (MIN): 90 ?

of Pitstops: 2 ?

Visualization

Power Consumption ?

Torque-Speed Curves ?

Power Overlay ?


Speed-Time ?

Fields in Bold are considered edit fields, while the plain text fields are calculated values.

Each panel in this window corresponds to a different aspect of the vehicle.

Help is available for each field to provide an explanation of how to use or interpret it with the press of the "?" button adjacent to the field.

Warning! the vehicle will not finish the race ?



This application is authored by Andrew Rivers.




Figure 2 Main Program Window with Help Buttons Marked as ‘?’

Users enter all parameters of their car design and track conditions in the main program window (the simulation control window) in order to run a simulation of the performance of Greenpower’s Formula 24 electric race cars. This menu driven interface allows students to manipulate design variables and observe the effect on outputs or performance indicators. The parameters are placed under suitably labeled sections in the window such as ‘Physical Dimensions’, ‘Motor Controller’ or ‘Race & Track Conditions’. All fields in bold are editable inputs to be adjusted for a simulation run. In addition to allowing all available parameters to be adjusted, the simulation control window shows outputs fields and allows plots to be viewed. Immediately upon startup and upon any input change, the simulation is rerun. This provides a snapshot of the vehicle’s performance within seconds of the input being changed. Below is a tabulation of the GUI inputs, outputs and functions that will be covered.

Table 1 Summary of GUI Components and Functions Covered

Summary of GUI Inputs, Outputs and Functions
<p>User-Specified Input parameters</p> <p>The following parameters can be varied</p> <p>Speed and Power</p> <ul style="list-style-type: none"> Drive Sprocket Driven Sprocket Motor Selection Motor Controller <p>Physical dimensions</p>

Body Style

Ride Height

Drag Coefficient

Frontal Area

Total Mass

Wheel Diameter

Tire Pressure

Innertube Type

Bearing Type

Battery

Brand

Series Connections

Parallel Connections

Minimum Battery Voltage

Battery State of Charge

Input/Output

Load Parameters

Save Parameters

Browse to File

Race and Track Conditions

Elevation Change

Custom Elevation Change

Number of Pitstops

Output and Visualization

The following are computed and displayed in response to change in input parameters

Power Consumption Plot

Torque-Speed Curves Plot

Power Overlay Plot

Speed-Time Plot

Drive Ratio

Maximum Speed

Required Motor Output Power

Required Motor Torque

Range

Acceleration Energy

Acceleration Time

Motor Regulation

Resistance Dominance

Motor Efficiency

Peak Motor Output Power

Motor Heat Output

Drag-Area

Current Draw
C-Rate
Watt-Hours Available
Discharge Time
Battery Side Power
Battery Side Voltage

3.2 Modeling and Derivation of GUI Outputs

The following sections detail models and derivation needed to produce the desired outputs. Wherever possible, empirical data was used to develop the models as it provides the best representation of the vehicle components in this case.

3.2.1 Wheels and Tires

Two of the most frequent mechanical concerns in motorsports aimed at increasing efficiency are physical mass and rolling resistance. Consequently, both terms appear in the GUI. Mass effects the vehicle's acceleration as well as rolling resistance, while tire construction and innertube choice directly influence the mechanical losses associated with rolling. Wheel sizes are restricted by the rules to be between 12" and 20" in diameter and must be made of metal [7]. Though complex tire models exist for determining more exact performance over broad rotational speed ranges and slip angles, a linear model is assumed here for the sake of simplicity. With the low power nature of the Greenpower cars causing them to operate at no to low slip angles the majority of a lap, the assumption of a constant coefficient of friction is a reasonably accurate

one. This constant coefficient of friction leads to a perfectly linear rolling resistance throughout the speed range. For a given load placed on the tire and a given rotational speed, the tire will dissipate power directly proportional to these two terms in accordance with Equation 2.

$$F_{roll} = C_{rr}N \quad (1)$$

$$P_{roll} = F_{roll} * \omega_{tire} \quad (2)$$

The coefficient of rolling resistance, C_{rr} , is taken from empirical tests conducted in [10] [11] and [12]. Though the specific tires tested are of a larger diameter than those used in Greenpower competition, extrapolation to the smaller size is straightforward. Consider the Schwalbe Durano tire tested in [11] was 28" in diameter consumed 18.0W at 18mph. The same model tire is legal in Greenpower competition in 20" form. To estimate the losses in the smaller tire, the ratio of diameters is taken and multiplied by the power consumption of the larger tire:

$\frac{28''}{20''} * 18W = 25.2W$. This linear assumption comes about from the tires having the same physical construction and proportions and therefore consuming approximately the same amount of energy per unit of circumferential rotation, i.e., the same coefficient of rolling resistance. This equivalently means that the frequency of the losses has increased for the smaller tire by exactly the ratio of the diameters. This assumption was used for both the Schwalbe Durano and Kojak tires to derive the coefficients of rolling resistance at different tire pressures.

The GUI also allows the selection of innertube type between traditional Butyl rubber tubes, Latex and Tubeless. Table 2 contains the differences in C_{rr} for each type at various pressures while Figure 3 is a graphical depiction of the data [10].

Table 2 Summary of Rolling Resistance Versus Tire Pressure for Different Innertubes

Tire Pressure (PSI)	Tubeless C_{rr}	Latex Tube C_{rr}	Butyl Tube C_{rr}
15	0.0061	0.0066	0.0084
25	0.0052	0.0055	0.0067
35	0.0049	0.0051	0.0060
45	0.0047	0.0048	0.0056
55	0.0046	0.0046	0.0054

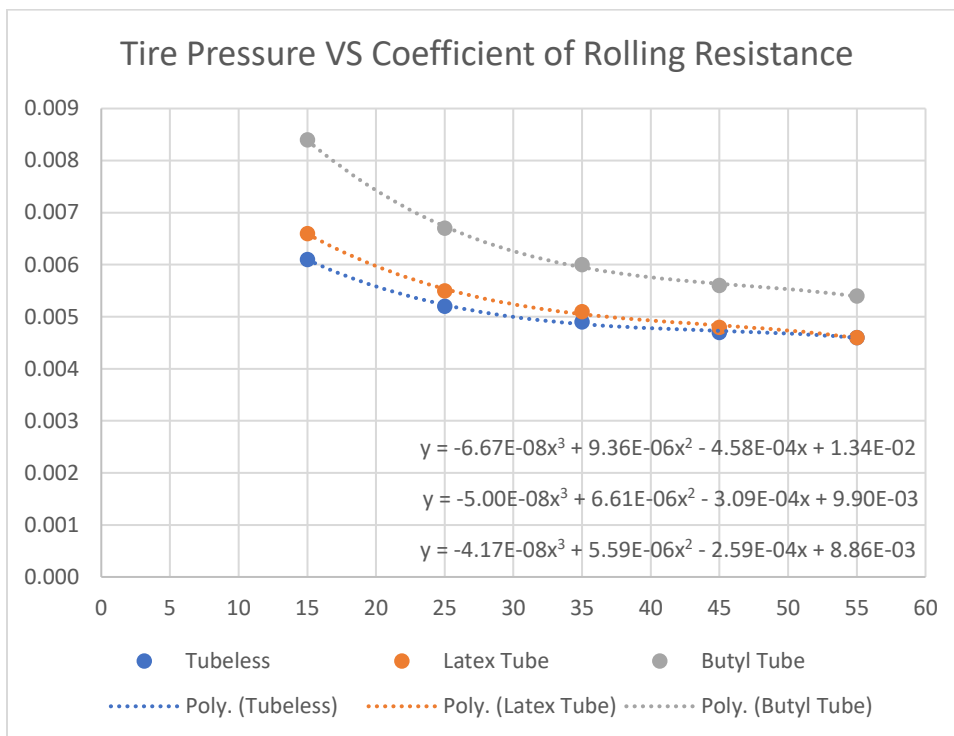


Figure 3 C_{rr} Dependence on Innertube

This raw data was then converted into delta values in Table 3 with the Butyl tube at 55PSI being the reference as it most closely represents the situation found in Greenpower Stock class cars [10]. This gives some intuition as to how much the C_{rr} changes as pressures and construction vary. Figure 4 is a graphical representation of the table [10].

Table 3 Difference in C_{rr} Based on Innertube and Pressure

Tire Pressure (PSI)	Tubeless ΔC_{rr}	Latex Tube ΔC_{rr}	Butyl Tube ΔC_{rr}
15	0.0007	0.0012	0.003
25	-0.0002	0.0001	0.0013
35	-0.0005	-0.0003	0.0006
45	-0.0007	-0.0006	0.0002
55	-0.0008	-0.0008	0

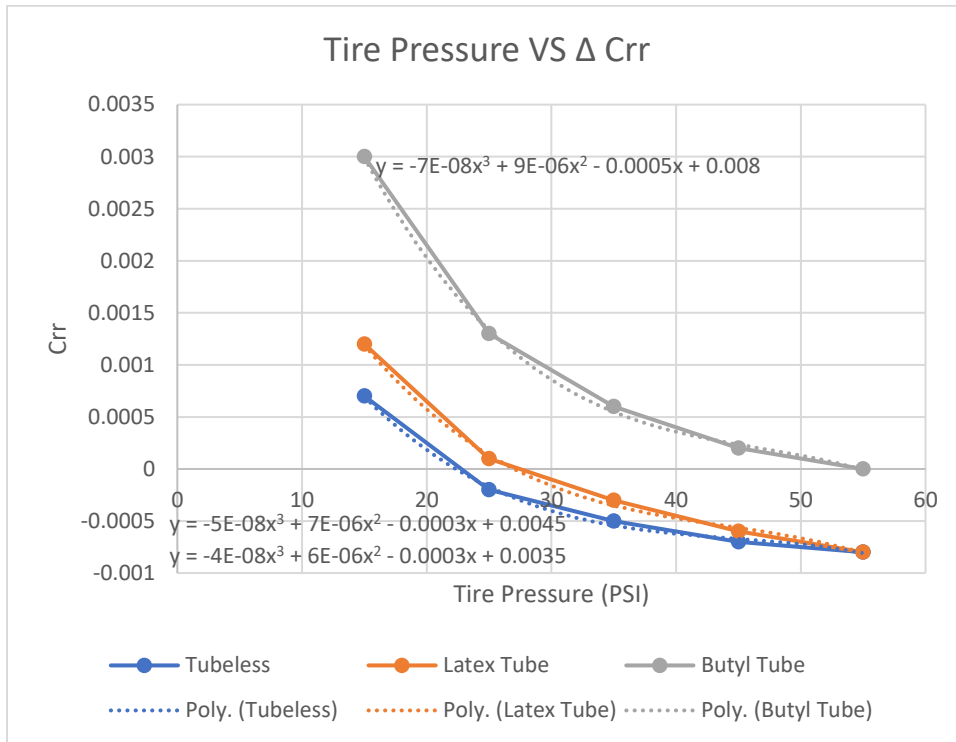


Figure 4 ΔC_{rr} Dependence on Innertube

This data is alternatively expressed as a percent change in Table 4. Positive values represent an increase in rolling resistance, while negative values represent a decrease [10].

Table 4 Percent Difference in C_{rr} Based on Innertube and Pressure

Tire Pressure (PSI)	Tubeless % Change	Latex Tube % Change	Butyl Tube % Change
15	12.963	22.222	55.556
25	-3.704	1.852	24.074
35	-9.259	-5.556	11.111
45	-12.963	-11.111	3.704
55	-14.815	-14.815	0.000

With knowledge of the third order polynomials describing the data trends, it was possible to have estimates of the coefficient of rolling resistance within the pressure range tested for each of the constructions. The percent changes are the values used in the user interface as the specific tire tested was not the same as what is used in Greenpower competition. This data is used to develop a trend in differing tube types. For the two specific Schwalbe tires sold on the Greenpower website, specific rolling resistance tests for these tires are cited. Beginning with the Schwalbe Kojak, Table 5 summarizes its coefficient of rolling resistance characteristics at various tire pressures [12].

Table 5 Schwalbe Kojak C_{rr} Versus Tire Pressure

Tire Pressure (PSI)	Coefficient of Rolling Resistance
30	0.01124
45	0.00872
60	0.00743
75	0.00656
90	0.00615

This data is plotted and fit to a polynomial in Figure 6 [11].

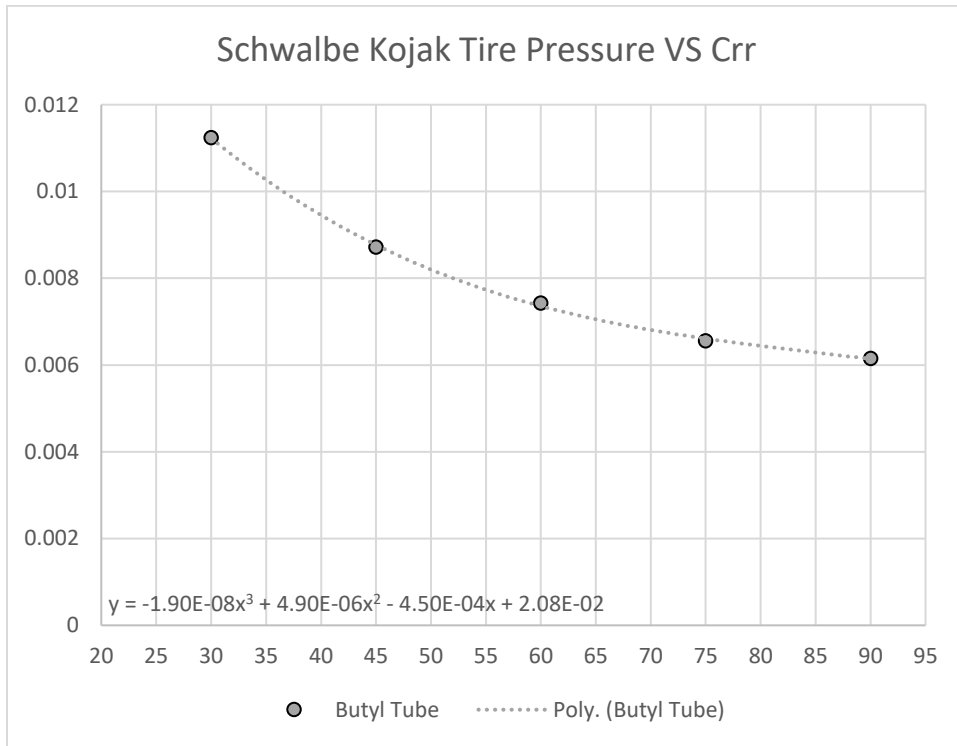


Figure 5 Schwalbe Kojak C_{rr} VS Tire Pressure

Table 6 Schwalbe Durano C_{rr} Versus Tire Pressure

Tire Pressure (PSI)	Coefficient of Rolling Resistance
60	0.00740
80	0.00629
100	0.00564
120	0.0054

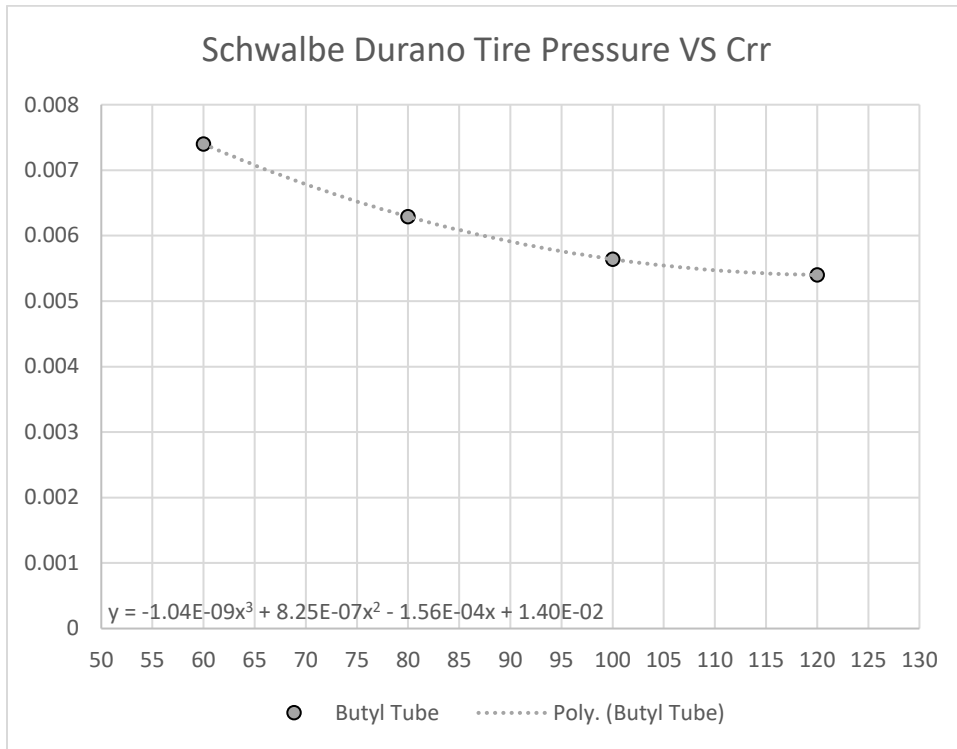


Figure 6 Schwalbe Durano C_{rr} VS Tire Pressure

The one datapoint these two tires have in common is at 60PSI. Using the polynomial that was fit to the data for the Kojak, an additional datapoint at 80PSI was obtained. Working in the reverse direction and fitting a polynomial to the Durano data of Table 6, datapoints at 75 and 90PSI were also added [11]. A comparison of these datapoints is available in Table 7 below [11] [12]:

Table 7 Common Data Points for the Schwalbe Kojak and Durano

Tire Pressure (PSI)	Schwalbe Kojak	Schwalbe Durano
60	0.00743	0.00740
75	0.00656	0.0065
80	0.0064	0.00629
90	0.00615	0.0059

Both Schwalbe tires share the Performance casing construction and mainly differ in tread thickness and design. The Kojak is 1.35” wide while the Durano is 1.10”. The similarities in construction cause the tires to have similar rolling resistance as evident in Figure 7 [11] [12].

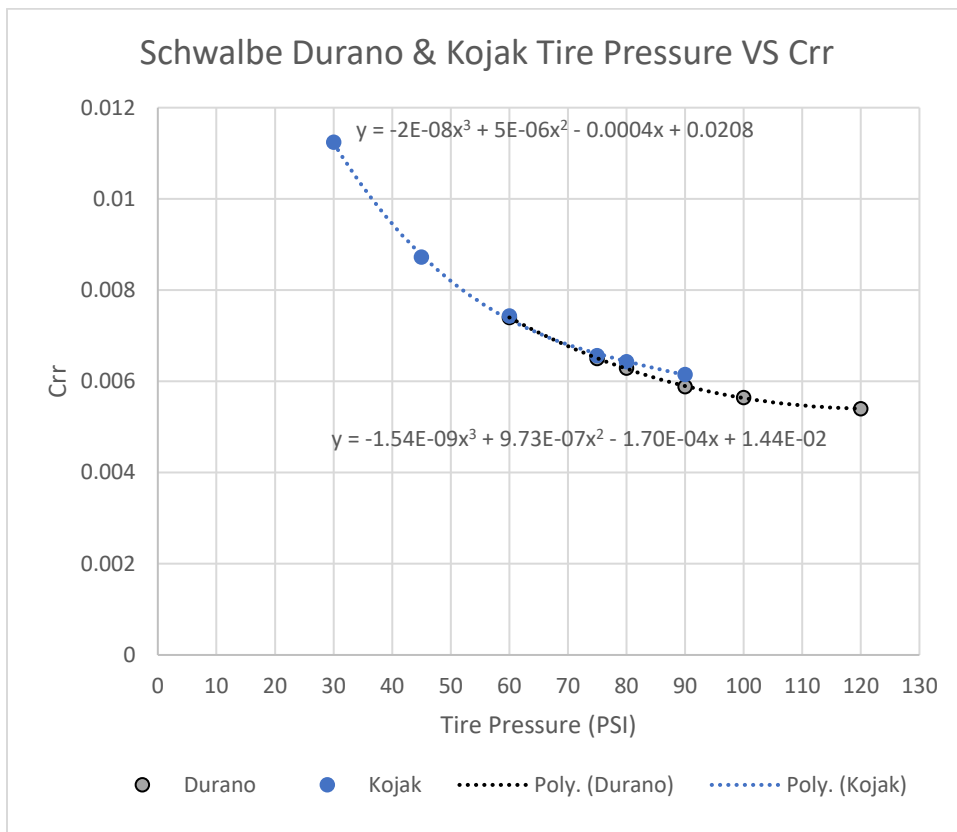


Figure 7 Comparison of C_{rr} for the Schwalbe Kojak and Durano Versus Tire Pressure

3.2.2 Motors

All Greenpower Formula 24 cars use low power, four pole, permanent magnet brushed DC motors for propulsion. Though not as common as they once were, the well-developed

literature and simplicity of DC machines make them a sound choice for low power machines [13]. Three generations of motors have been used in the Greenpower competitions since its inaugural season in 1999. Each generation of motor has the same power, voltage, and speed ratings and therefore any of the three approved motors are legal in present day competition. The first of these motors was produced by the FRACMO company in the UK. Its performance is depicted in Figure 8 below [14]:

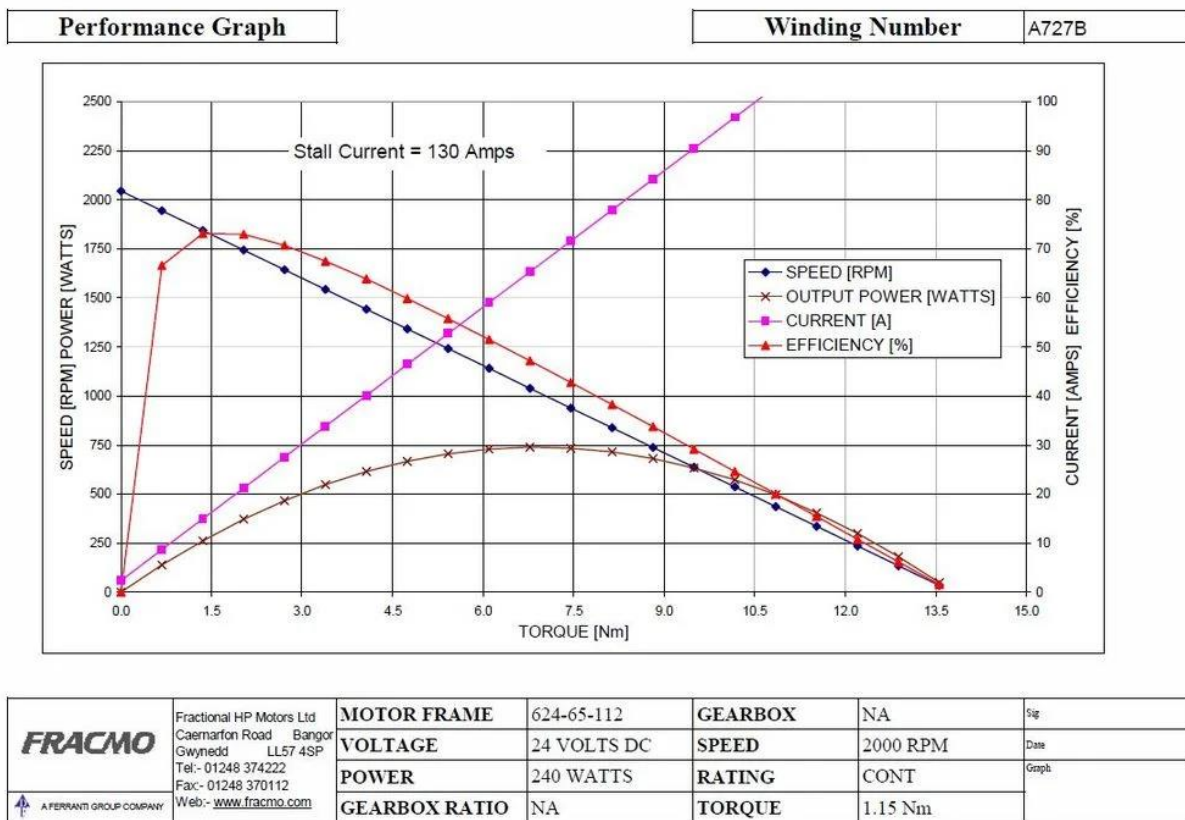


Figure 8 FRACMO Motor Characteristic Curves

One of the popular motor controllers used in the modified and custom categories of F24 is 4QD. Their website provides a partial performance curve family for the latest generation of Greenpower motor, as seen below in Figure 10 [15].

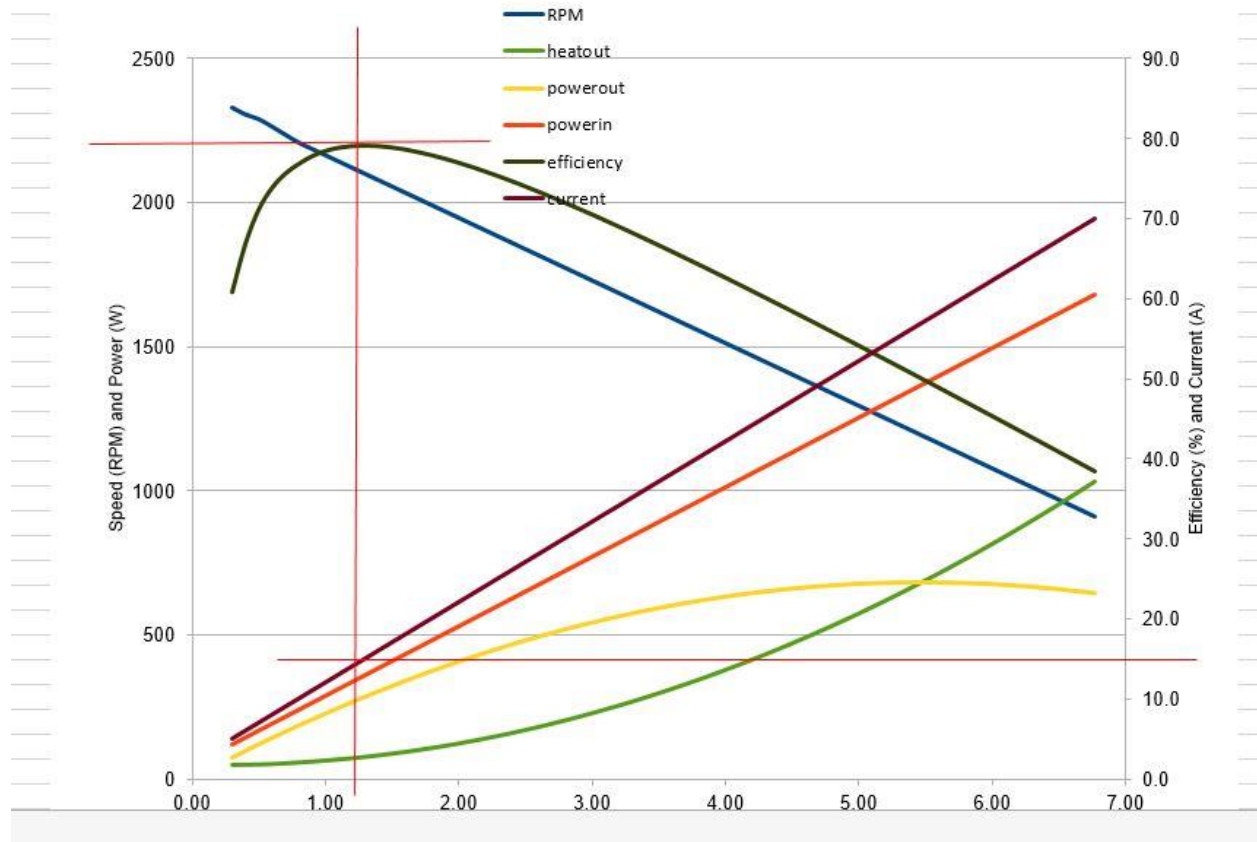


Figure 9 Shanbo EM Motor Characteristic Curves

To determine the power output of the motor, Equation 3 is used.

$$P = \tau\omega \quad (3)$$

The power output of the motor is equal to the rotational speed, ω , multiplied by the electromagnetic torque, τ .

$$\tau = K_t I \quad (4)$$

The torque generated by a permanent magnet brushed DC motor is directly proportional to the current through the armature. The factor K_t is known as the torque constant of the motor and is expressed in Nm/A.

$$K_t = K_{t_{20}} \left(1 + \alpha_{magnet} (T_f - 20) \right) \quad (5) [16]$$

Equation 5 above determines the torque constant of the motor at a given temperature T_f . Because the measurements to determine the speed and torque constants were taken at 20°C, the scale is shifted by this value. The temperature coefficient of the ferrite (Ceramic) magnets used in the Greenpower motors, α_{magnet} , is -0.0020/°C [16]. This means the magnets lose 0.2% of their strength every 1°C increase in temperature. Though this may appear negligible at first, consider just a 10°C rise in motor case temperature and the motor constants have changed by a full 2%, meaning the motor now develops 2% less torque and will rotate 2% faster than it did previously under no load. Considering the motors used in Greenpower F24 cars are often run near their rating, they may experience a temperature rise of at least 19°C, based on testing in Chapter 4, resulting in a significant performance change. An alternative way to consider how this change will affect the performance of the car is to observe the motor regulation, the slope of the torque speed curve. When placing the motor under a given load, the motor will naturally decrease in speed until the applied torque is equal to the output torque. When the output torque is decreased for a given input current, the motor must slow further to provide the required level of torque.

$$K_e = 1/K_t \quad (6)$$

When expressed in Newton-meters per Ampere, the speed constant of the motor K_e is the inverse of the torque constant.

In the GUI, the default motor selected is the third-generation motor, the Shanbo EM. This

automatically loads the K_e and K_t values for that motor at 20°C and then uses Equation 5 to adjust the constants based on the temperature input by the user.

3.2.3 Gearing

The F24 cars are traditionally equipped with a single stage roller-chain reduction drive, though other forms of power transmission are permitted in the Modified and Custom categories. In the F24 Stock category, the drive ratio is 12:72 or 1:6, drive to driven. This means every six turns of the motor; the drive wheel turns one revolution. There is a tendency for larger sprockets to produce slightly higher efficiency due in part to the reduced pinch angle of the chain¹⁰. This effect is presently neglected, and the user may input the drive efficiency manually, or use the default value of 95%. The efficiency gains to be had by increasing the diameter of the sprockets for a given ratio are small. In a 1998 article in the 2nd International Conference on the Engineering of Sport titled “Improving cycling performance with large sprockets”, Burgess, S.C. conducted a test on a bicycle with two identical gear ratios [17]. The difference, however, was that one set of sprockets were twice the diameter of the other, the smaller pair being 13T and 26T and the larger pair 26T and 52T. With this test setup, Burgess was able to measure an increase in efficiency of 0.6%, up to 99.4% from 98.8%, with the larger sprockets¹⁰. Though doubling the size of the sprockets on the Greenpower cars is not practical for the kit-based setups due to space constraints, it could be feasible for Custom class cars.

3.2.4 Motor Control

In the Stock class of F24, there are no motor controllers permitted. In this case, the driver controls the speed of the car with a contactor directly connecting the 24V battery to the motor. This binary form of control only permits one stable cruising speed, maximum. Though efficient

and relatively simple to model, this form of control does not allow the driver to select a potentially more optimal speed to maintain. However, many teams who compete in categories allowing motor controllers do not use them. The additional cost, complexity and electrical losses are all cited as being obstacles which must be overcome.

3.2.5 Battery

Lead-acid batteries are a low-cost, high-power option for low-speed electric vehicles [18]. All Greenpower Formula 24 cars are powered by a pair of 12V, Absorbent Glass Mat (AGM) lead-acid batteries wired in series. Section T2 states of the technical regulations for Formula 24 states, these two batteries are to be the sole source of stored energy for propelling the car ¹³. It is therefore necessary to operate the battery in an efficient manner to ensure the maximum energy may be extracted from it. In general, this means keeping the discharge current as low as possible. Peukert's Law is one method of expressing how well a battery maintains capacity under different loads. The Peukert constant, k , is a dimensionless exponent which describes how the battery loses capacity. The closer the constant is to unity, the less capacity the battery loses. Typical values for lead acid battery chemistries range from 1.1-1.3 [19]. The forms of Peukert's Law used in this work are expressed in equations 7 and 8 below.

$$t = H \left(\frac{C}{IH} \right)^k \quad (7) [19]$$

Solving Eq.7 for the Peukert Constant k , yields:

$$k = \frac{\ln\left(\frac{t}{H}\right)}{\ln\left(\frac{C}{IH}\right)} \quad (8)$$

Where H is the discharge time at the rated capacity, t is the actual discharge time, C is the rated

capacity, and I is the constant current (CC) draw during time t.

The two approved batteries for use in Greenpower Competition are the Interstate DCM0035 and the Yuasa REC36-12. A datasheet for the Interstate battery is not publicly available and an equivalent battery from AJC, part number AJC-D35S, was used as a reference. Figures 11 through 14 give information as provided by the manufacturer’s datasheet [20] [21].

Product Specification

Voltage	12V	Weight	Approx. 11.2kg
Capacity	36Ah @ 20hr-rate	Max. Discharge Current	360A (5 sec)
Operating Temperature Range	Discharge: -15°C–45°C Charge: -15°C–45°C Storage: -15°C–45°C	Internal Resistance	Approx. 8.7mΩ
Normal Operating Temperature Range	25±2°C	Container Material	A.B.S (UL94HB)
Terminal	Bolt M5 Tightening torque 2.0–3.0Nm (20–30kgf · cm)		
Dimensions	Length: 196±2mm Width: 130±2mm	Case Height: 158±3mm Overall Height: 169±3mm	

Figure 10 Yuasa Battery Specifications

Discharge Capacity

Constant Current Discharge Characteristics: Watts (25°C)

F.V./ TIME	5M	10M	15M	20M	30M	45M	1H	2H	3H	4H	5H	10H	20H
10.8V	1200	860	690	569	428	317	253.4	147.9	105.6	84.5	71.8	38.4	20.7
10.5V	1270	920	714	584	436	320	254.2	148.4	106.0	84.8	72.0	38.6	20.9
10.2V	1350	970	733	596	442	322	254.5	148.9	106.6	85.2	72.4	38.8	21.1
9.6V	1470	1000	746	604	446	324	255.0	150.6	108.2	86.6	73.6	39.5	21.2

Constant Current Discharge Characteristics: Amps (25°C)

F.V./ TIME	5M	10M	15M	20M	30M	45M	1H	2H	3H	4H	5H	10H	20H
10.8V	107	76	59	49.2	36.8	27.1	21.5	12.41	8.80	7.04	5.98	3.19	1.78
10.5V	115	82	62	50.8	37.6	27.4	21.6	12.46	8.85	7.08	6.02	3.21	1.80
10.2V	124	88	64	52.1	38.3	27.7	21.6	12.48	8.87	7.09	6.03	3.22	1.81
9.6V	139	91	66	52.9	38.8	27.9	21.7	12.63	9.01	7.21	6.13	3.28	1.81

Figure 11 Yuasa Discharge Characteristics

- Specifications

Nominal Voltage		12V
Rated Capacity 77 ⁰ F(25 ⁰ C) (10HR)		35.0Ah
Dimensions (mm/inch)	Length	195 (7.68)
	Width	130 (5.12)
	Height	155 (6.10)
	Total Height	180 (7.09)
Approx. Weight (kg/lbs)		9.6 (21.16)
Terminal		T8/T11

- Characteristic

Capacity 77 ⁰ F(25 ⁰ C)	20HR (1.855A)	37.1Ah
	10HR (3.500A)	35.0Ah
	5HR (5.950A)	29.8Ah
	1HR (19.25A)	19.3Ah
	15 min rate (61.25A)	15.3Ah
Internal Resistance	Full Charged Battery 77 ⁰ F(25 ⁰ C)	Approx. 8m Ω
Temperature dependence of capacity (10HR)	104 ⁰ F(40 ⁰ C)	102%
	77 ⁰ F(25 ⁰ C)	100%
	32 ⁰ F(0 ⁰ C)	85%
	5 ⁰ F(-15 ⁰ C)	65%
Self-Discharge 68 ⁰ F(20 ⁰ C) (Capacity after)	3 months	90%
	6 months	80%
	12 months	60%
Max. Discharge Current, 77 ⁰ F(25 ⁰ C)		350A(5s)
Floating design life, 77 ⁰ F(25 ⁰ C)		10 years
Constant Voltage Charge, 77 ⁰ F(25 ⁰ C)	Cycle	14.4~14.7V(-24mV/ ⁰ C) max. current: 8.75 A
	Float	13.6~13.8V(-18mV/ ⁰ C)

Figure 12 AJC-D35S Battery Specifications

Constant Current Discharge Characteristics (A), 77°F(25°C)

F.V/TIME	5min	10min	15min	30min	60min	2H	3H	5H	8H	10H	20H
1.60V/cell	119.0	77.0	61.2	35.0	20.3	12.61	9.29	6.28	4.20	3.65	1.91
1.70V/cell	113.1	73.2	58.5	33.5	19.6	12.13	9.09	6.16	4.15	3.61	1.89
1.75V/cell	107.8	68.6	65.7	32.8	19.3	11.90	8.91	6.06	4.07	3.55	1.88
1.80V/cell	101.2	63.4	56.4	32.2	18.9	11.70	8.75	5.95	4.03	3.50	1.86

Constant Wattage Discharge Characteristics (Watt), 77°F(25°C)

F.V/TIME	5min	10min	15min	30min	60min	2H	3H	5H	8H	10H	20H
1.60V/cell	211.2	139.9	112.2	64.4	37.6	23.54	17.50	11.94	8.05	7.12	3.73
1.70V/cell	202.6	134.1	108.2	62.2	36.6	22.84	17.26	11.82	8.01	7.09	3.72
1.75V/cell	194.9	126.9	107.2	61.5	36.3	22.61	17.06	11.71	7.95	7.04	3.72
1.80V/cell	184.6	118.2	106.3	60.8	36.0	22.41	16.86	11.61	7.91	7.00	3.71

Figure 13 AJC-D35S Discharge Characteristics

Comparison of the two batteries [20] [21]:

Table 8 Comparison of Battery Capacity Ratings and Internal Resistance

	AJC-D35S	Yuasa REC36-12
20HR Rate Capacity (AH)	37.1	36
Internal Resistance (mΩ)	8	8.7

Using the rated capacity values at 20 hours, the constant current draw at different discharge times and the reported capacity at each discharge rate from the datasheets, the Peukert Constants could be calculated with Equation 8. Summarized in Table 9 are the discharge rates and times for the two batteries. Discharge rates above and below the 90-minute requirement were calculated to give an accurate curve fit for the desired range.

Another parameter considered by this battery model is the sag in voltage from the resistive component of the battery.

Table 9 Peukert Constants of the AJC and Yuasa Batteries

CC Discharge Time (Hours)	Current Draw (A)	AJC-D35S Peukert Constants	Current Draw (A)	Yuasa REC36-12 Peukert Constants
0.083	107.8	1.349	115	1.318
0.167	68.6	1.326	82	1.254
0.25	56.7	1.281	62	1.238
0.5	32.8	1.248	37.6	1.226
1	19.3	1.279	21.6	1.214
2	11.9	1.239	12.46	1.206
3	8.91	1.210	8.85	1.206

Using the open circuit voltage of the battery as a reference, the voltage drop across the resistive component is calculated with equation 9.

$$V_{sag} = V_{SOC} - IR \quad (9)$$

Where V_{SOC} is the open circuit voltage of the battery at a particular state of charge. I is the current through the batter, equal to the motor current in the controllerless case presented here, and R is the internal resistance of the battery. Changes in internal resistance due to heat, state of charge level and battery age are neglected at this point in the work. Figure 14 depicts the voltage dependance on SOC of a 6 cell AGM battery [22].

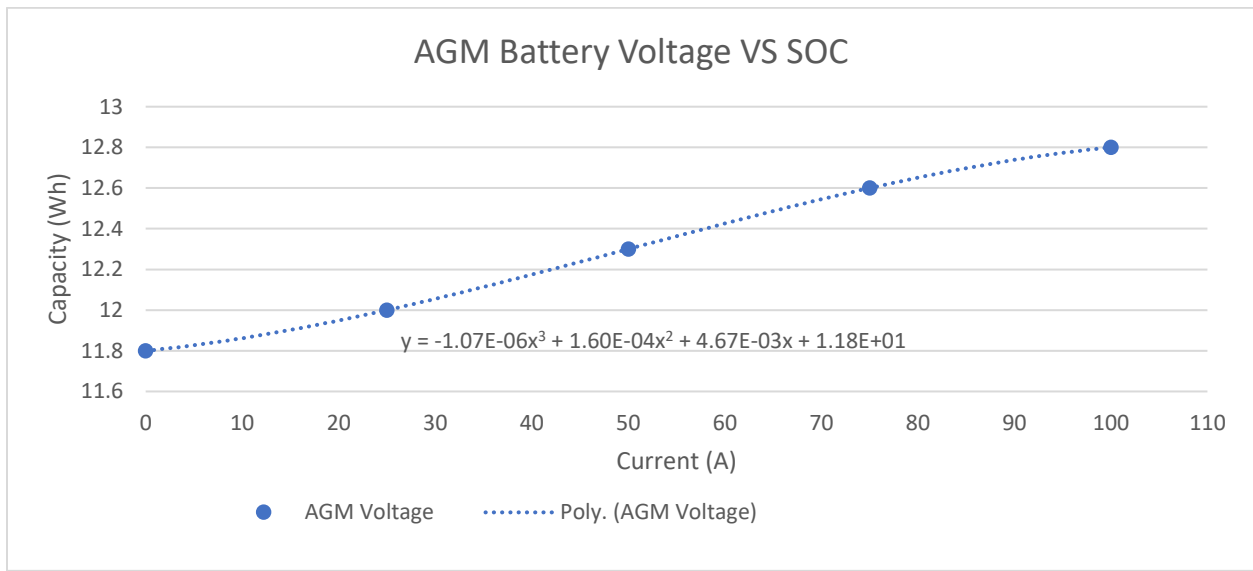


Figure 14 Battery Voltage VS State of Charge

To expand the use of this work into future rule changes and other, similar forms of motorsport, such as Electrathon, the number of series and parallel connected batteries can be input by the user. If the team is using a battery management system, the minimum battery voltage may also be selected.

3.2.6 Aerodynamics

Computational Fluid Dynamics (CFD) is growing to be more common in school competitions involving fluid flow. With the use of Simscale's Free software, it was possible to determine a starting point for the drag area of a basic Formula 24 Car. A simplified CAD model of the car was prepared in OnShape. The dimensions of the model were taken from the Siemens SolidEdge model which is provided to the teams free of charge.

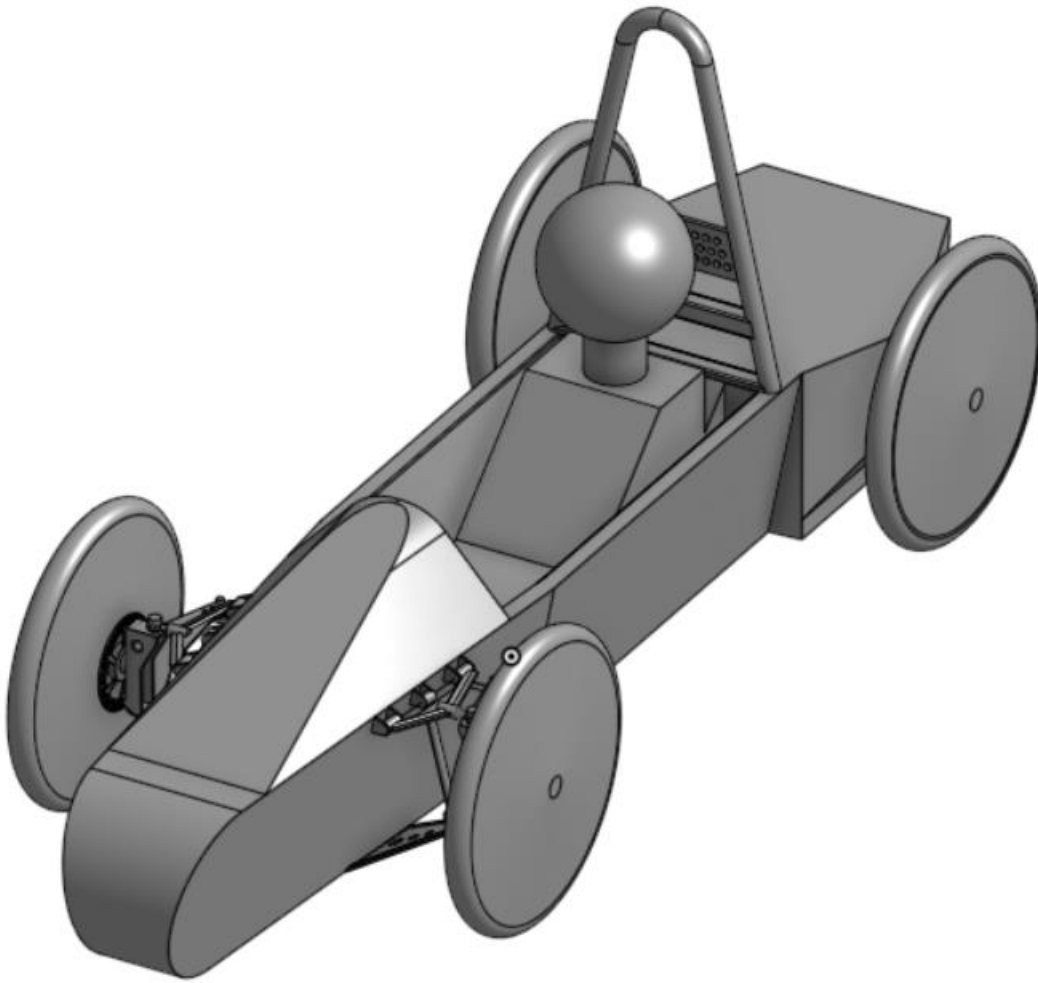


Figure 15 Simplified CAD Model ¾ View

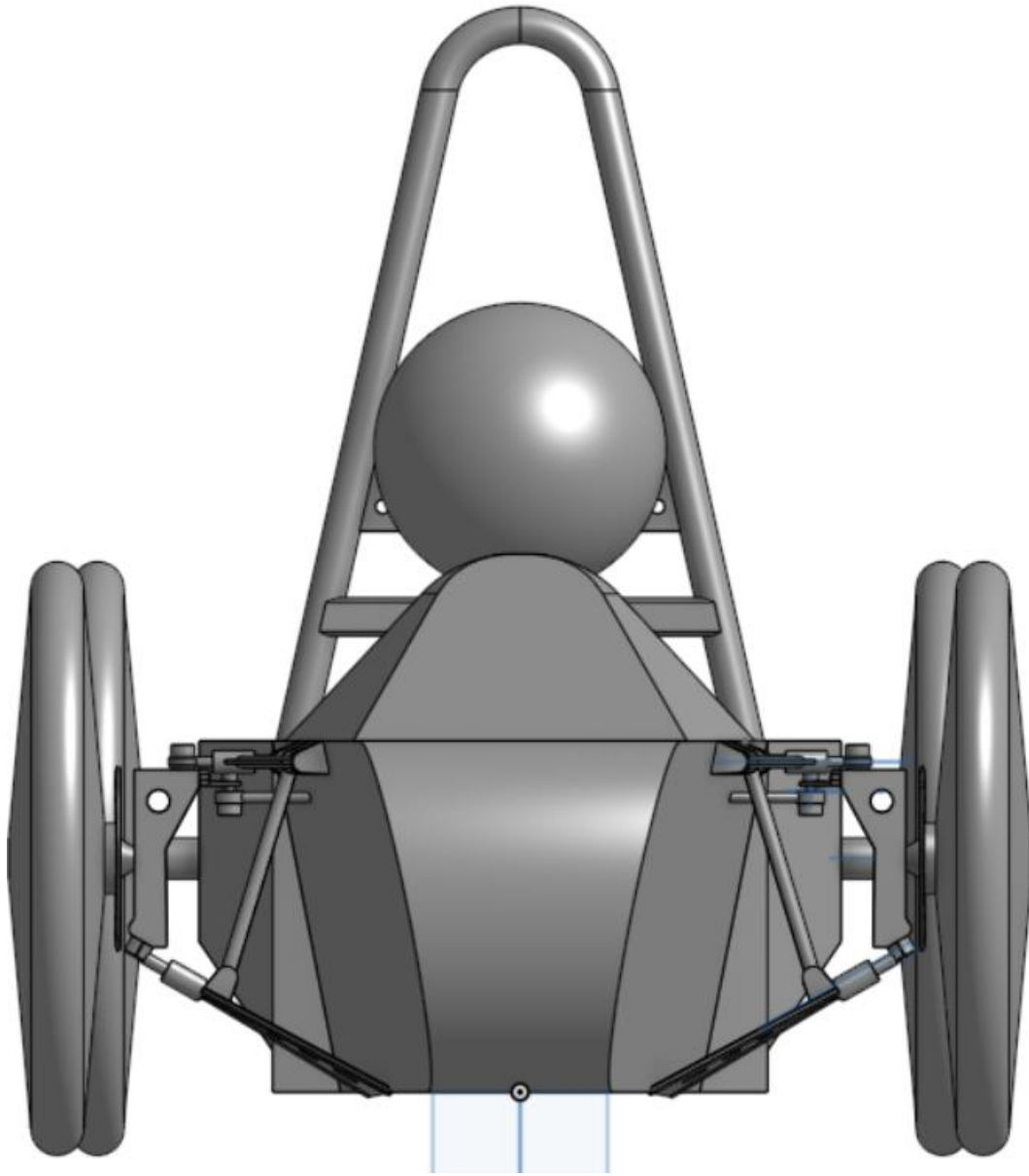


Figure 16 Simplified CAD Model Front View

The well-known equations of a body moving through a viscous fluid are as follows:

$$F_{drag} = \frac{1}{2} \rho C_d A V^2 \quad (10)$$

$$P_{drag} = \frac{1}{2} \rho C_d A V^3 = F_{drag} V \quad (11)$$

Where F_{drag} is the force the fluid exerts on the body in Newtons. ρ is the density of the fluid, and the terms C_d , A , and V are the drag coefficient, frontal area and velocity of the body respectively. P_{drag} is the power consumed by F_{drag} over some distance and time. The density of air was assumed to be that of Standard Temperature and Pressure (STP) as $1.225 \frac{kg}{m^3}$.

Aerodynamics are a crucial consideration when efficiency is concerned as even small velocities can produce large power requirements with the cubic nature of the function. The Greenpower cars are often characterized by relatively small frontal areas and relatively high drag coefficients when compared to the average streetcar. This leads to the drag area, or $C_d A$, being a better judge of aerodynamic resistance than simply one of the terms.

Three free versions of software were used in the creation of the aerodynamic model of a typical Greenpower car. The first software, Siemens SolidEdge, was used to obtain the physical dimensions of the car's frame. This information was then translated into a simplified OnShape solid model for use in SimScale's Finite Element Analysis tools. The SolidEdge model was not used directly as it is unnecessarily detailed for CFD analysis. Once the OnShape model was completed, it was imported directly into SimScale, as this feature is supported in SimScale. The model, now in SimScale, then had a cartesian box drawn around the car such that the centerline of the car was coplanar with one face of the box. This allows only one half of the vehicle to be simulated along a symmetric axis and saves computation time. Figure 18 shows the guidelines followed to dimension the bounding box, where L is the length of the body under test [23]. This "virtual wind tunnel" created by the cartesian box is then used to create a mesh of the volume. Refinements around the vehicle body were used to enhance the detail of the flow around the surfaces and in the wake region.

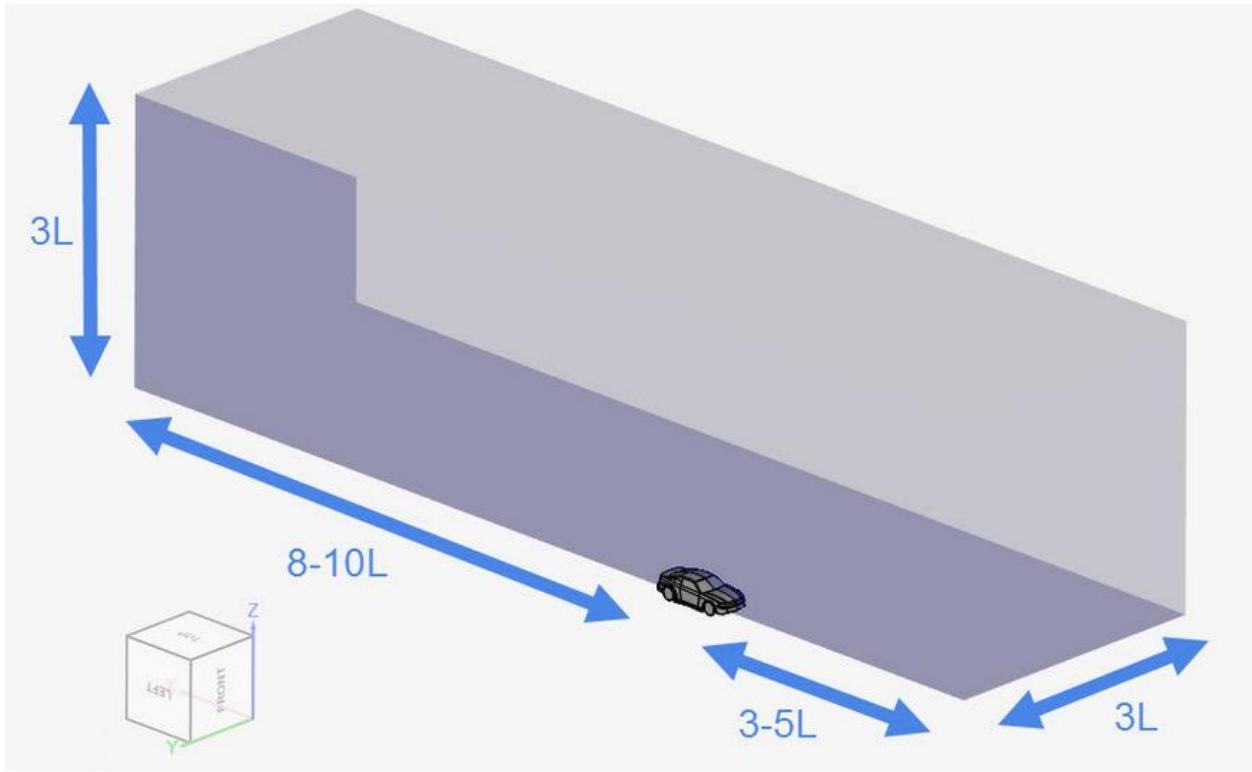


Figure 17 Boundary Cartesian Box Dimensions

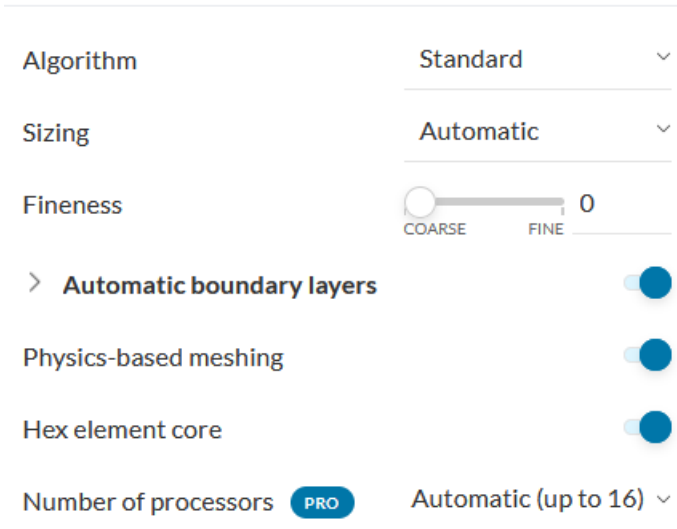


Figure 18 CFD Mesh Settings

The mesh was generated with the settings seen above in Figure 19. In all regions outside the refinements, the mesh was made as coarse as possible to reduce computation time without sacrificing flow detail around the body. Cylindrical and rectangular refinement regions were defined to completely enclose the vehicle and driver. The refinements are referred to in maximum edge length of a cell inside the region. A single large box encompassing the vehicle and the wake region used an edge length of 0.02m, while the regions immediately surrounding the body were made to be 0.005m. This ensured accurate meshing of the more detailed features of the body and prevents excessive jagged edges while allowing the wake region to have a coarser mesh.

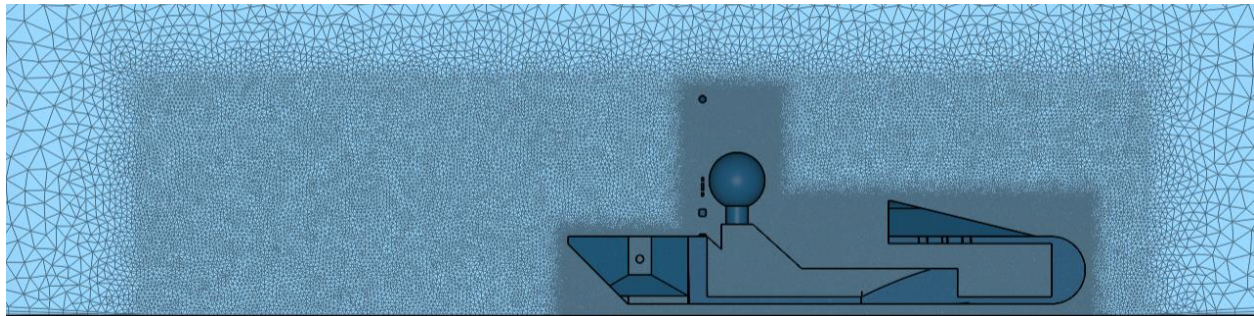


Figure 19 Cross Section of Mesh Depicting Refinements

The drag coefficient resulting from this simulation was 0.58 while the frontal area was approximately $0.36m^2$.

3.2.7 Force and Power

To begin the simulation, constants and initial vectors are first loaded into the startup function. Wherever possible, the vectors are made to be the same length to improve consistency

when viewing plots and to allow the matrix algebra to be completed between them. The startup function then makes all necessary calculations from the previous sections to display a starting point on the main program window. Because the tires are the only point of contact for the driving force of the vehicle, they are considered first. The circumference of the tire is calculated based on the user selection of wheel size and is then paired with the no-load speed of the motor at the given temperature to determine the range of speeds the car can obtain under its own power. Once this range is established, an array of power consumption values is calculated based on the aerodynamic drag rolling resistance and drivetrain efficiency. This provides the knowledge of how much energy is consumed to maintain all possible speeds of the car. Once this is known, the array can be divided by the rotational speed of the wheels to determine the torque at the drive wheel. This can then be used to back out the torque at the motor output shaft by dividing by the drive to driven gear ratio. This motor torque, designated the required motor torque, is used to calculate the required current through the armature based on the torque constant. A separate current vector is used in the battery calculations to provide an array of battery output voltages and effective capacities at each motor torque. This current vector is based on the stall current of the motor and consists of equally spaced points from the No Load Current (NLC) to stall. This vector does not start at zero due to there being no torque production to maintain rotation against losses at that current. Motor efficiency and armature joule heat production are also calculated at this stage. The aforementioned required motor torque is then compared to the possible motor torque at a rotational velocity that would produce the speed associated with that required torque. The vectors are compared and as soon as the required torque exceeds the available torque, the previous index of the vector is recorded. This previous index indicates where in the current vector the torque capabilities are still feasibly able to drive the vehicle forward. Ideally, a point is

found where the required and available torques are identical as this provides the maximum speed the vehicle can drive on level ground. The length of the vectors is therefore made to be large, at least equal to the maximum speed of the fastest generation of motor in RPM, in this case 2400RPM, in an effort to reduce errors due to the step size. Now that the actual maximum speed of the vehicle is known, and its index within each of the vectors, the power consumed at that exact speed can be calculated as well as the kinetic energy of the entire vehicle. Acceleration time is determined by the time it takes to build the kinetic energy in each step along the speed vector. Because this simulation is presently done assuming no motor controller is used, the motor response is to a step function. With this in mind, the maximum power is applied to the motor at all points during an acceleration from a standstill to maximum speed. It is therefore possible to simply subtract the required motor power from the available motor output power. This power delta gives the available power to accelerate the car, similar to the swing equation in power generation. The kinetic energy vector holds the values of the entire vehicle's kinetic energy at every point along the speed vector. Power, being the dividend of energy and time, can then be found by dividing the kinetic energy by the power delta, gives the time it takes to make each step in kinetic energy $\frac{J}{s} = s$. The resulting vector of time is then cumulatively summed, and the scalar result is the time necessary to make all of the steps in kinetic energy up to the maximum speed.

3.2.8 Output Plots

The user interface features a set of three buttons under the “Visualization” panel. The three plots depicting power consumption, torque-speed characterization and available versus required power and efficiency, are shown below:

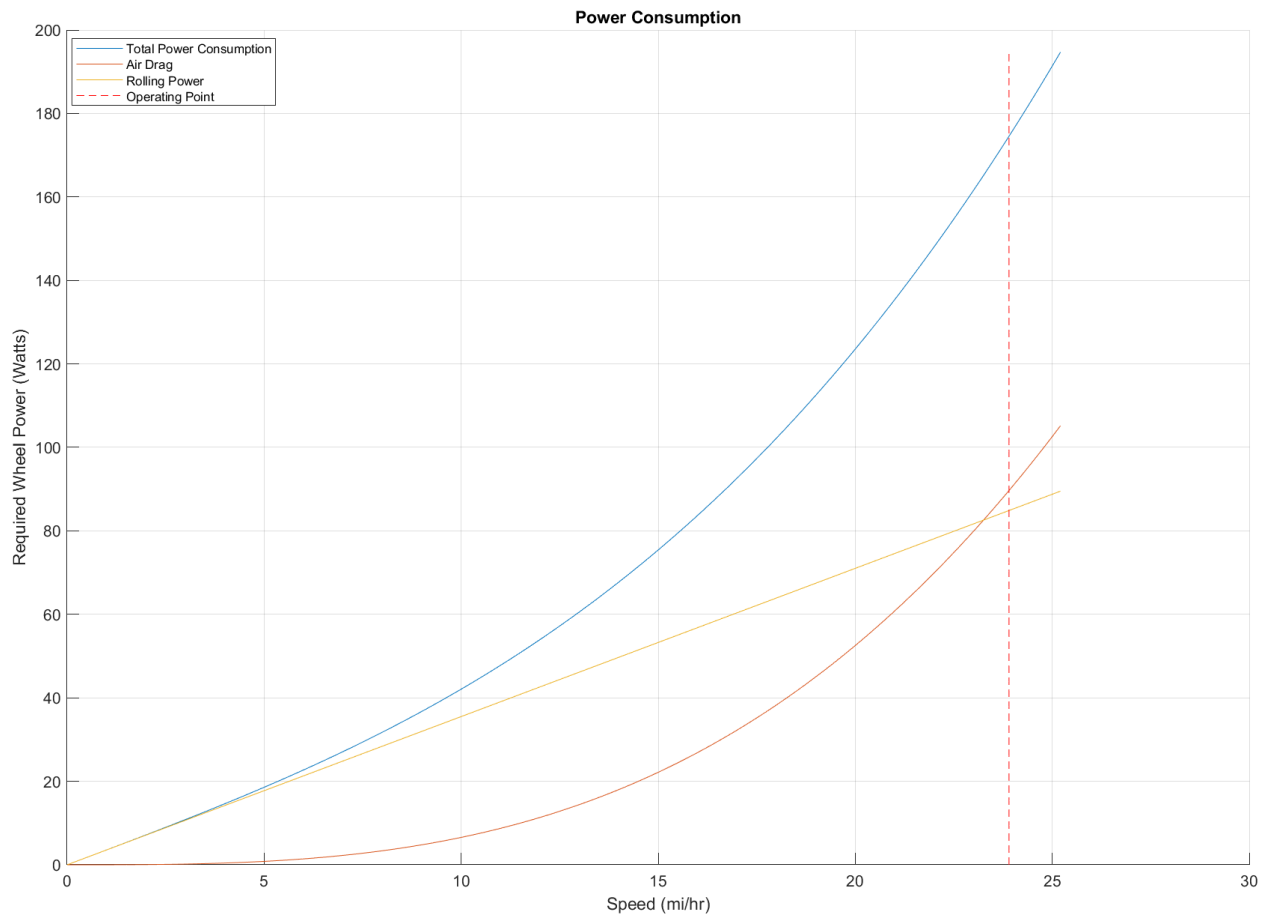


Figure 20 Power Consumption of the Car

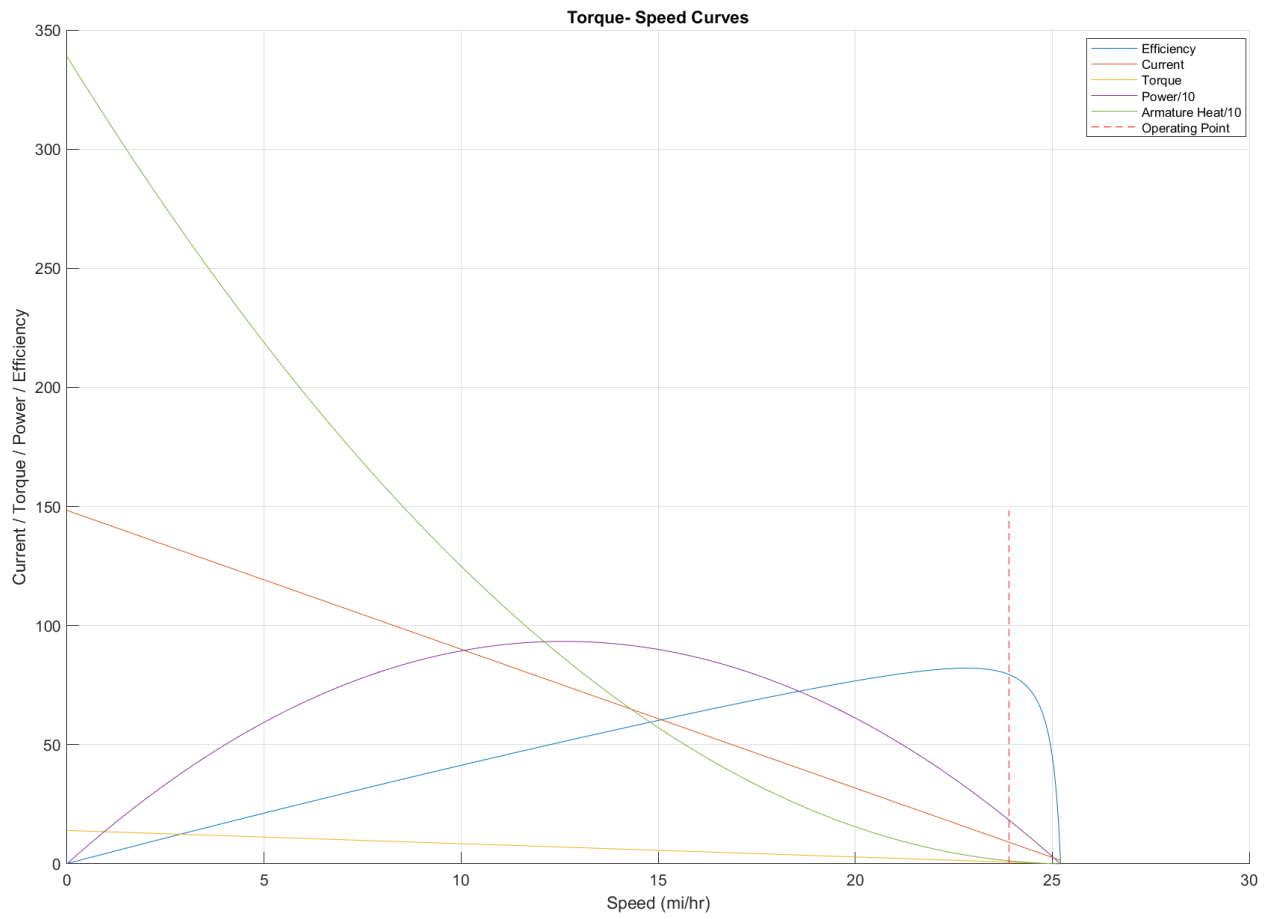


Figure 21 Characteristic Curves of the Shanbo Greenpower Motor

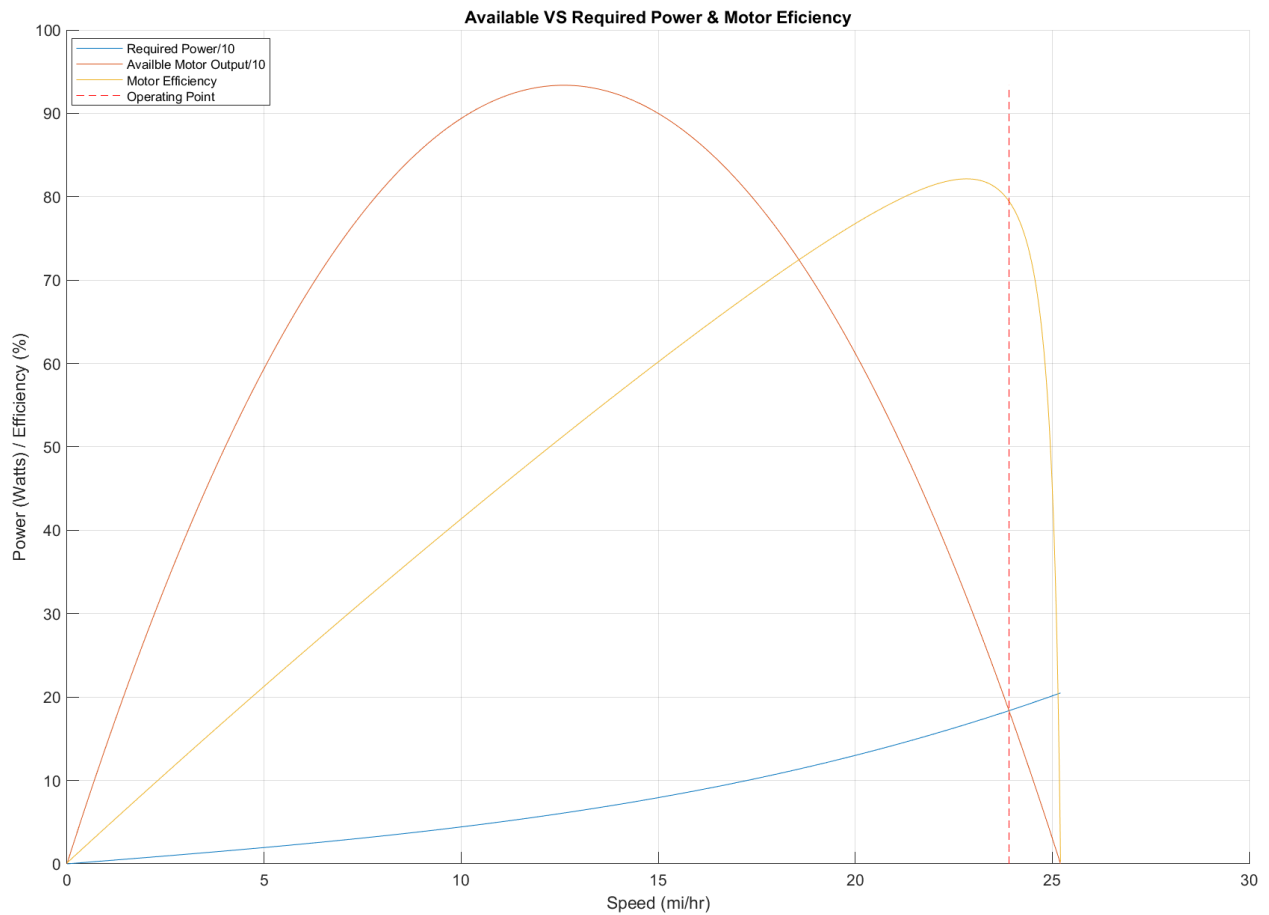


Figure 22 Overlay of Required Power, Motor Power and Motor Efficiency

3.2.9 Numeric Output Fields

- This section gives an overview of the output fields seen in the main application window and how each of them was obtained.
- The Drive Ratio is simply the ratio of the driven to drive sprocket tooth counts. It is an indication of how many times the motor must turn for a single rotation of the rear wheel.

- The Maximum Speed field displays how fast the car can travel on level ground for the given set of conditions defined by the input fields.
- Required Motor Output is equal to the sum of all losses divided by the efficiency of the chain drive. This gives the load as seen by the motor output shaft.
- Similar to the Required Motor Output, the Required Torque is the rotational force the motor must produce to maintain that maximum speed.
- The Range numeric output field displays the distance the car could travel assuming maximum speed is maintained.
- Acceleration Energy is the number of watt-hours consumed in an acceleration event from stationary to maximum speed. This is what is experienced at the start of a race and after each pit stop.
- The 0-Max Speed Time field displays the time it takes to reach maximum speed when starting from a stand still.
- Motor Regulation is the decrease in rotational speed of the motor relative to the applied load torque. This field is directly dependent on the temperature of the motor.
- Resistance dominance lets the user know which of the two main forces, rolling resistance or aerodynamic drag, acting on the car are dominant at the maximum speed.
- Motor Efficiency displays the value of the motor efficiency at the maximum speed of the vehicle.

- Peak Motor Output is the maximum power output the motor is capable of producing under the given set of conditions.
- Max Motor RPM shows the motor speed corresponding to maximum vehicle speed.
- Motor Heat Output is the power dissipated from copper losses in the motor at maximum vehicle speed.
- The CdA of the car, also known as the drag-area, is the product of the drag coefficient and the frontal area.
- The Current draw numeric field displays the number of amps required to maintain maximum vehicle speed.
- The C-Rate of the battery is the current draw of the previous field divided by the amp-hour rating of the battery.
- Wh Available is the energy capacity of the battery when loaded at maximum speed.
- The Discharge time is the time it would take to drain the battery from the present state of charge to zero capacity.
- Battery Side power, though equivalent to motor side power when not using a motor controller, is the power drawn from the battery in order to maintain maximum speed.
- Battery Side Voltage accounts for any voltage sag in the battery due to current draw as well as the state of charge of the battery.

3.2.10 Help Functions

Each item in the main program window is paired with a question mark button immediately to its right. When pressed, a dialogue box appears on screen with additional information on how to use an input or how to interpret a result.

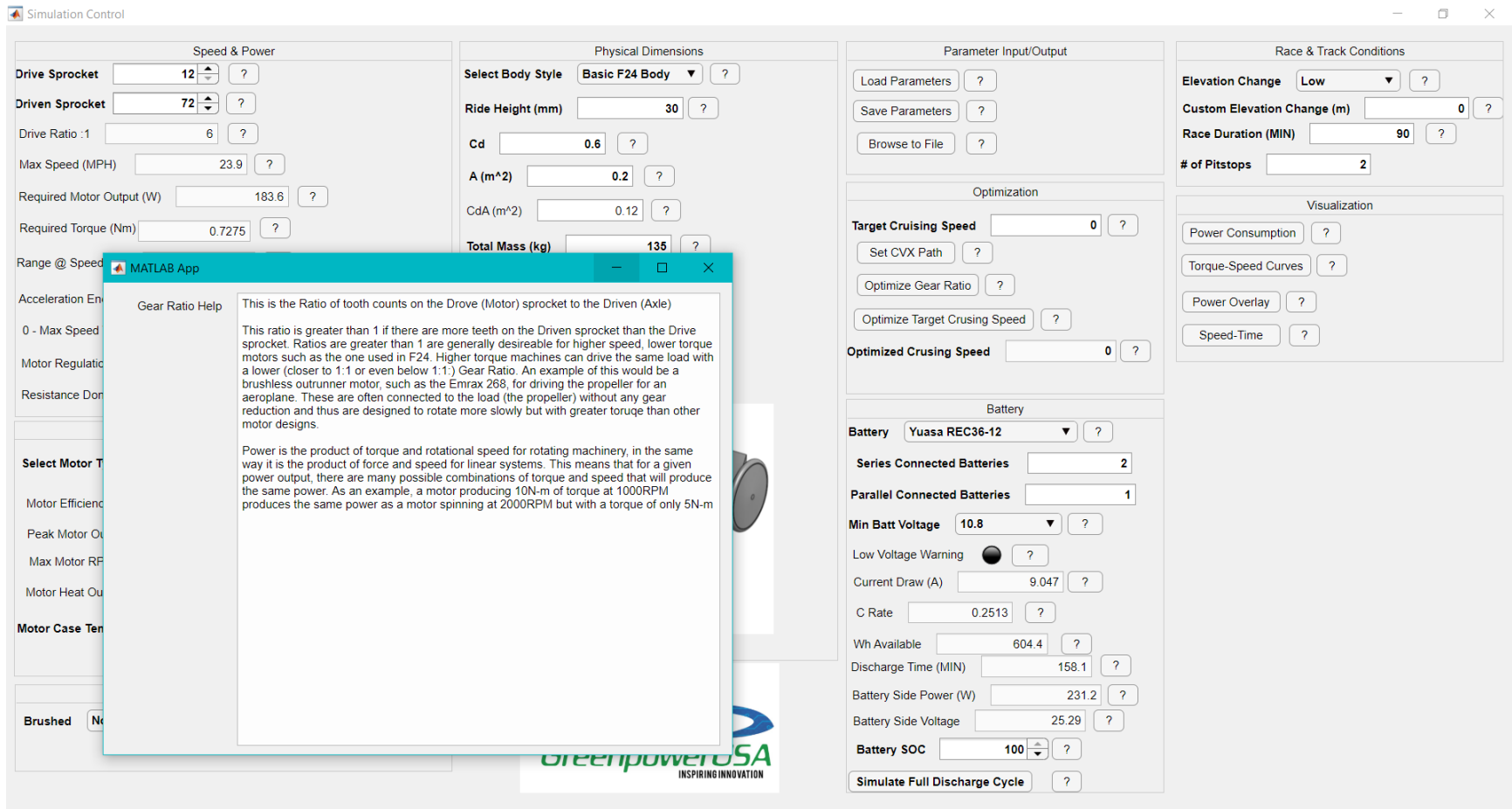


Figure 23 Help Dialogue

CHAPTER IV

EXPERIMENTAL TESTING

This chapter presents the experimental tests conducted to support the development of the models used in the GUI. Testing of the actual hardware used in competition provided an element of practical application currently missing. The details provided serve as a guide to those recreating the test conditions for their specific machines and as a reference for testing future generations of hardware.

4.1 Machine Ratings

This section begins with a summary of the machines used in experimental testing as part of model creation. The motors studied were all approved for use in Greenpower competition. Each of the three motors have the same general ratings summarized in Table 10 below:

Table 10 Greenpower Motor Nameplate Ratings

Parameter	Greenpower Motor
Rated Power (W)	240
Rated Voltage (V)	24
Rated Speed (RPM)	2000
Rated Current (A)	17
Rated Torque (Nm)	1.15

Both the 1st generation and 3rd generation motor use Class F insulation (155°C), while the 2nd generation motor has Class H (180°C) insulation on the armature windings.

Table 11 Motor Solver Generator Nameplate Ratings

Parameter	Motorsolver Generator
Rated Power (W)	250
Rated Voltage (V)	42
Rated Speed (RPM)	4000
Rated Current (A)	6
Rated Torque (Nm)	0.57
No Load Current (A)	0.97
Speed Constant V/kRPM	8.7
Terminal Resistance (Ω)	3.9
Terminal Inductance (mH)	0.665

4.2 Motor Armature Resistance

The resistance of each motor was experimentally determined at eight different armature positions and then averaged. To accomplish this, the armature was stalled, and the bench supply was operated in constant current mode at the maximum current of 6.15A. The position of the motor was determined based on the location of the flat on the output shaft. With the motor at room temperature, 20°C, the motor was stalled with the flat positions changing in approximately 45 mechanical degrees increments, starting with the flat facing upwards.

Table 12 FRACMO Armature Resistance

1 st Generation Motor (FRACMO 624-65-112)			
	Applied Voltage (V)	Current (A)	Resistance (Ω)
Position 1	1.600	6.15	0.260
Position 2	1.550	6.15	0.252
Position 3	1.500	6.15	0.244
Position 4	1.700	6.15	0.276
Position 5	1.650	6.15	0.268
Position 6	1.600	6.15	0.260
Position 7	1.800	6.15	0.293
Position 8	1.600	6.15	0.260
Average Armature Resistance			0.264

Table 13 Motion Tech Armature Resistance

2 nd Generation Motor (Motion Technologies DCA5N242024DL000)			
	Applied Voltage (V)	Current (A)	Resistance (Ω)
Position 1	1.200	6.15	0.195
Position 2	1.190	6.15	0.193
Position 3	1.250	6.15	0.203
Position 4	1.150	6.15	0.187
Position 5	1.300	6.15	0.211
Position 6	1.000	6.15	0.163
Position 7	1.300	6.15	0.211
Position 8	1.150	6.15	0.187
Average Armature Resistance			0.194

Table 14 Shanbo EM Armature Resistance

3 rd Generation Motor (Shanbo EM 105ZDY08)			
	Applied Voltage (V)	Current (A)	Resistance (Ω)
Position 1	1.000	6.15	0.163
Position 2	0.950	6.15	0.154
Position 3	0.970	6.15	0.158
Position 4	0.900	6.15	0.146
Position 5	1.000	6.15	0.163
Position 6	0.875	6.15	0.142
Position 7	0.900	6.15	0.146
Position 8	1.000	6.15	0.163
Average Armature Resistance			0.154

4.3 Motor Armature Inductance

Terminal inductance was also experimentally determined for each of the three motors utilizing Tektronix Application Note “Capacitance and Inductance Measurements Using an Oscilloscope and a Function Generator” [24]. This application note provides a method of measuring capacitance and inductance with a 3-5% uncertainty. The function generator used, though a different model than the one in the application note, also had a 50Ω output impedance, R_{fg} , and was capable of producing the desired sine wave signal. In accordance with the application note, the value of R_{ref} was experimentally adjusted to suite the inductance being measured. The reference resistance was adjusted until the 10kHz signal was resulting in an inductance measurement within 3% of the 0.665mH nameplate value of the Motorsolver generator. It was found that at approximately 450X the measured armature resistance, the best measurement for inductance was obtained. Utilizing this factor, the reference resistance was adjusted with a potentiometer for each of the three motors. Another deviation from the application note was in the use of a $5V_{p-p}$ signal rather than the $2V_{p-p}$ suggested. This was due to the relatively small resistance of the motor armature producing a correspondingly small voltage

drop at measurement point A2 in the figure. This small voltage drop, approximately 30mV, meant that a sizeable measurement error could be incurred with only 1mV of error. By increasing the signal voltage to 5V and decreasing the reference resistance to just 450X that of the armature, the voltage at A2 was increased to over 500mV, thus making it much easier to obtain a reliable amplitude reading. The measurement circuit can be seen in Figure 24 [24].

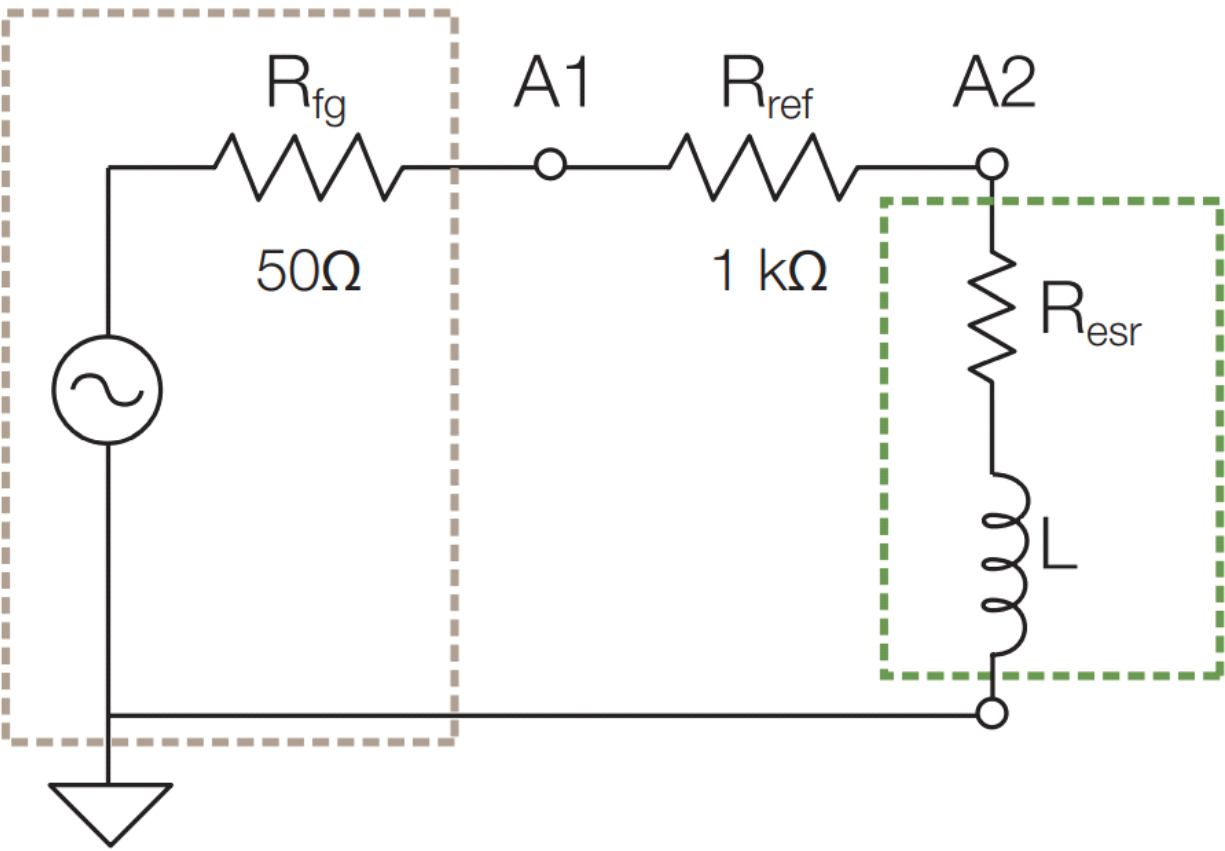


Figure 24 Schematic for Inductance Measurement

The inductance of each motor armature is summarized below in Table 15

Table 15 Summary of Armature Inductances

Motor Inductance Measurements			
	1 st Generation Motor (FRACMO 624-65-112)	2 nd Generation Motor (Motion Technologies DCA5N242024DL000)	3 rd Generation Motor (Shanbo EM 105ZDY08)
Inductance (μH)	239	240	172

4.4 Swinburn Tests

Due to the stator flux in permanent magnet DC machines remaining nearly constant, the use of a Swinburn test is applicable and precise for low current levels [25]. The Swinburn test, also known as the no-load or losses method is a way of determining the approximate efficiency of a motor or generator without the use of a dynamometer [25]. Instead, the motor or generator is powered under no load and the input power is measured. The no-load condition is of concern because it provides insight into the power loss in the motor or generator. Because under steady-state no-load conditions all of the input power is lost, this gives an estimate of the power loss in the machine throughout the speed range. Subtracting the Copper losses, I^2R , gives the remaining, dominantly mechanical losses including friction, windage and eddy current losses in the core. Plotting these datapoints over the speed range of the Greenpower motors results in the following:

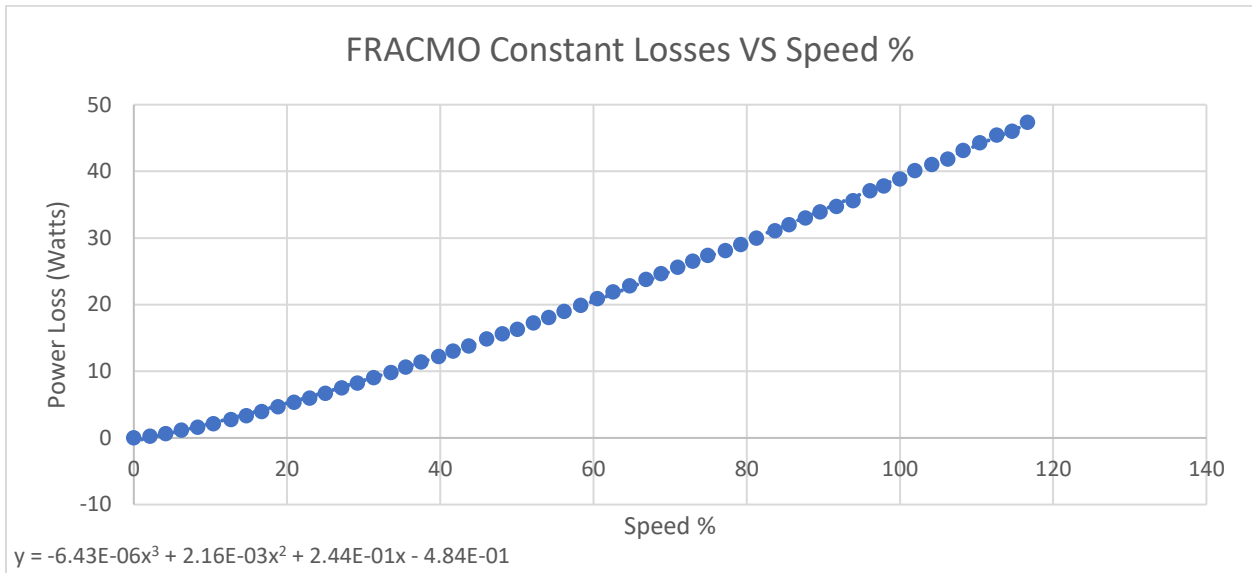


Figure 25 FRACMO Constant Power Loss VS Speed

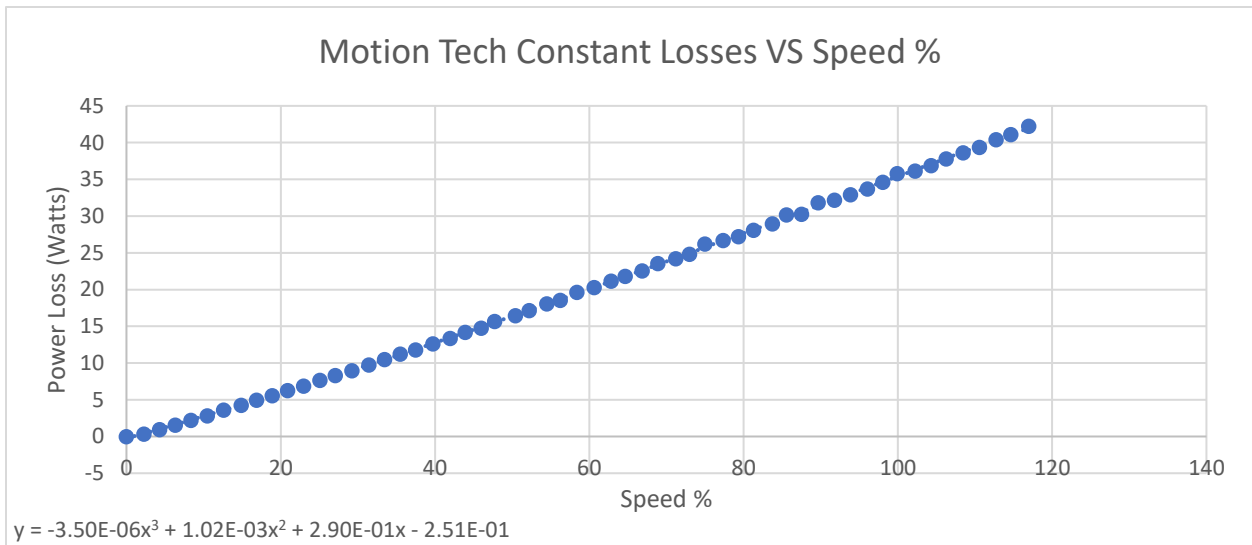


Figure 26 Motion Tech Constant Power Loss VS Speed

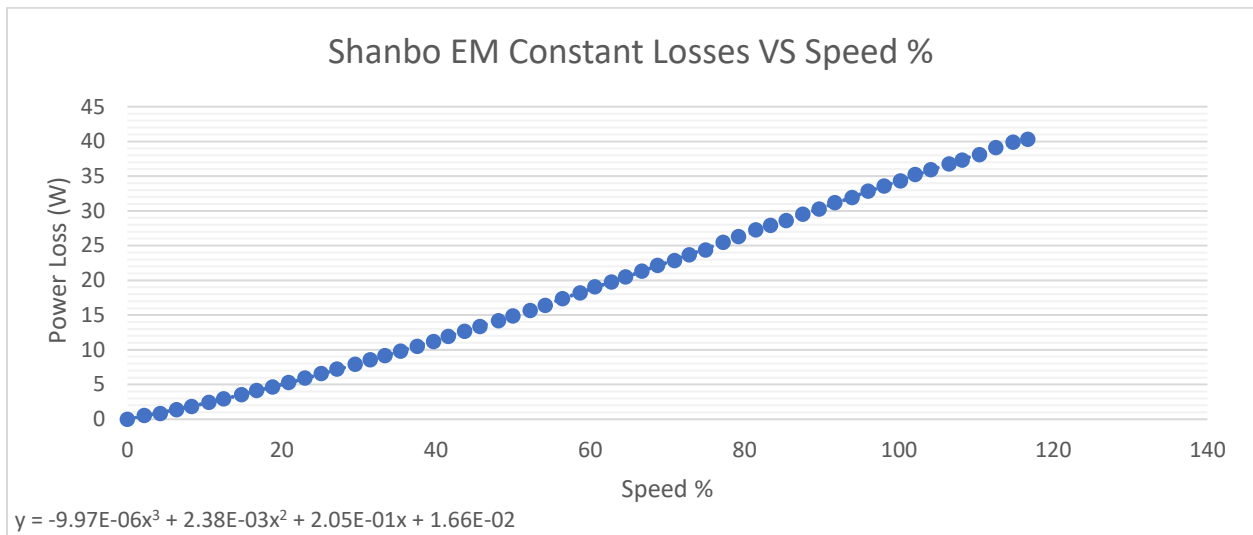


Figure 27 Shanbo EM Constant Power Loss VS Speed

This test was conducted on all three generations of Greenpower motors from zero to full battery voltage of 28v with the use of a TENMA 72-7245 power supply and two multimeters, one measuring current and the other the terminal voltage. A TENMA 72-1015 Multimeter was used to measure the current through the armature while a handheld BK Precision 2709B measured the terminal voltage. The maximum speed percentage is approximately 117% as the motors are rated at 24V and up to 28V was applied. Each step in voltage was approximately 0.5V providing 56 data points for each motor. At each voltage step, the terminal voltage and current were recorded, thus giving the power input to the motor and therefore the losses at each speed. As evident from the previous figures, the losses in the motors range from 40W to 48W maximum. This is approximately 1/6th of the rated power of the motors, neglecting the hysteresis iron losses. This leads to an efficiency cap of 1-40W/240W or 83.3% for the most efficient motor and 1-48W/240W = 80.0% for the least. To obtain approximate efficiency plots for each motor,

the copper losses were estimated at each current and added to the constant losses. To reiterate, these efficiency plots neglect hysteresis losses in the core and are therefore optimistic at higher loads.

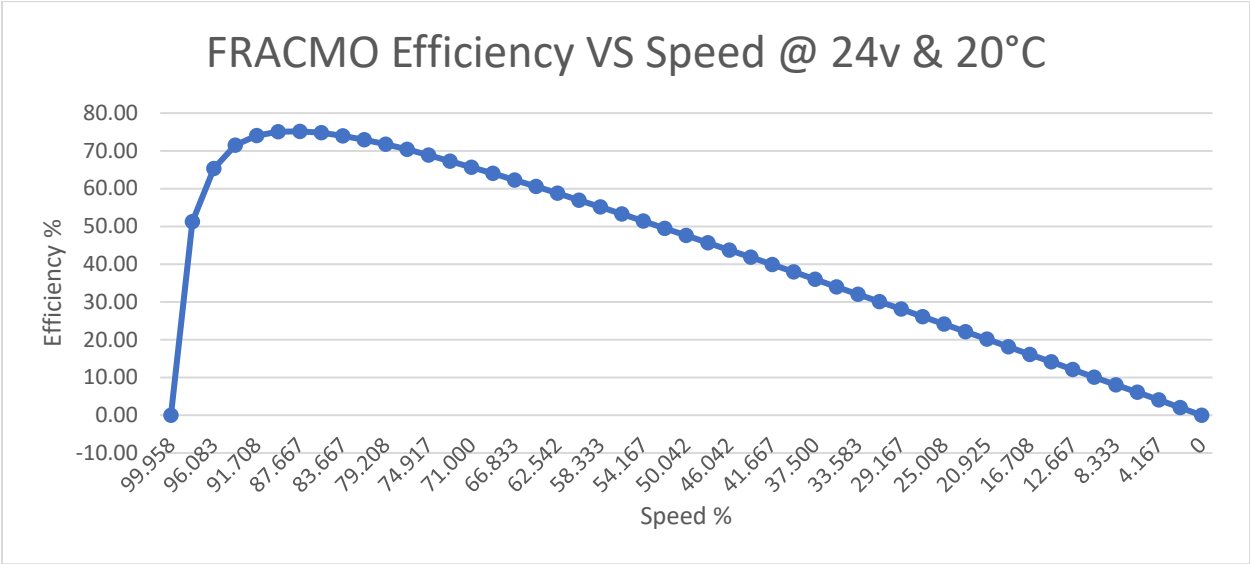


Figure 28 FRACMO Efficiency Versus Speed

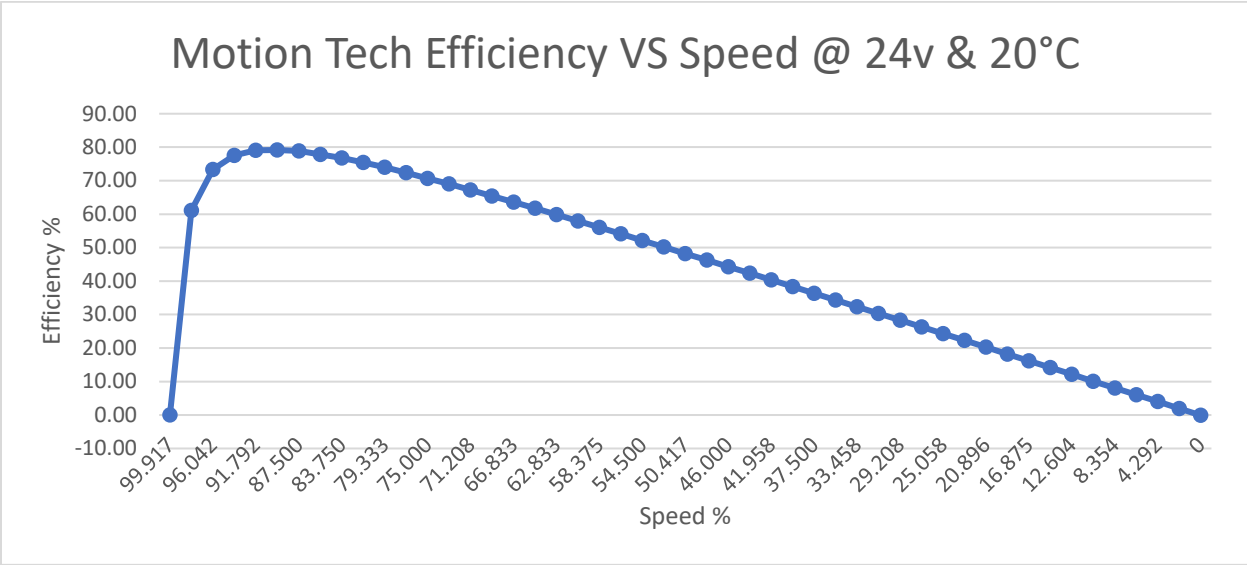


Figure 29 Motion Tech Efficiency Versus Speed

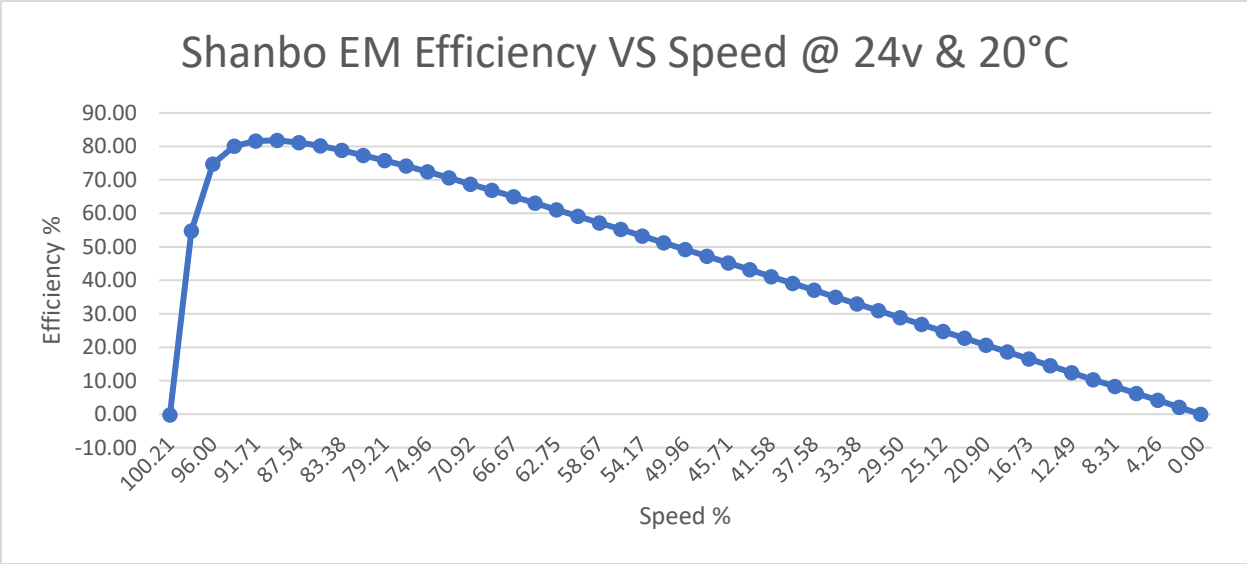


Figure 30 Shanbo EM Efficiency Versus Speed

Table 16 Summary of Motor Efficiencies

	1 st Generation Motor (FRACMO 624-65-112)	2 nd Generation Motor (Motion Technologies DCA5N242024DL000)	3 rd Generation Motor (Shanbo EM 105ZDY08)
Peak Efficiency (%)	75.17	79.16	81.81
Average Efficiency (%)	42.64	44.07	44.93

Table 17 Summary of No-Load Currents

	1 st Generation Motor (FRACMO 624-65-112)	2 nd Generation Motor (Motion Technologies DCA5N242024DL000)	3 rd Generation Motor (Shanbo EM 105ZDY08)
No Load Current (Amps)	1.65	1.51	1.44

4.5 Determining No-Load Speed, Torque-Speed Characteristics and Motor Regulation

In order to accurately model the brushed DC motors used in competition, knowledge of the no-load speed is necessary. However, the Greenpower motors are not fitted with encoders. To overcome this, an adapter for the 0.5” output shaft of the generator to the 20mm shaft of the motor was designed and 3D printed. In order to accurately and securely locate the motor in place on the dynamometer frame, an adapter was also designed, and 3D printed. The Motorsolver generator is equipped with a 1000 pulse-per-revolution (PPR) Timken M15 magnetic encoder and pulse readings from this were read on a Tektronix TDS 2002B oscilloscope. The motor was connected to the TENMA 72-7245 power supply, which was set to 24V and verified by the TENMA 72-1015 Multimeter. With the generator under open circuit conditions, only the mechanical resistance of the generator was loading the motor. A tabular result of this test can be found in Table 18.

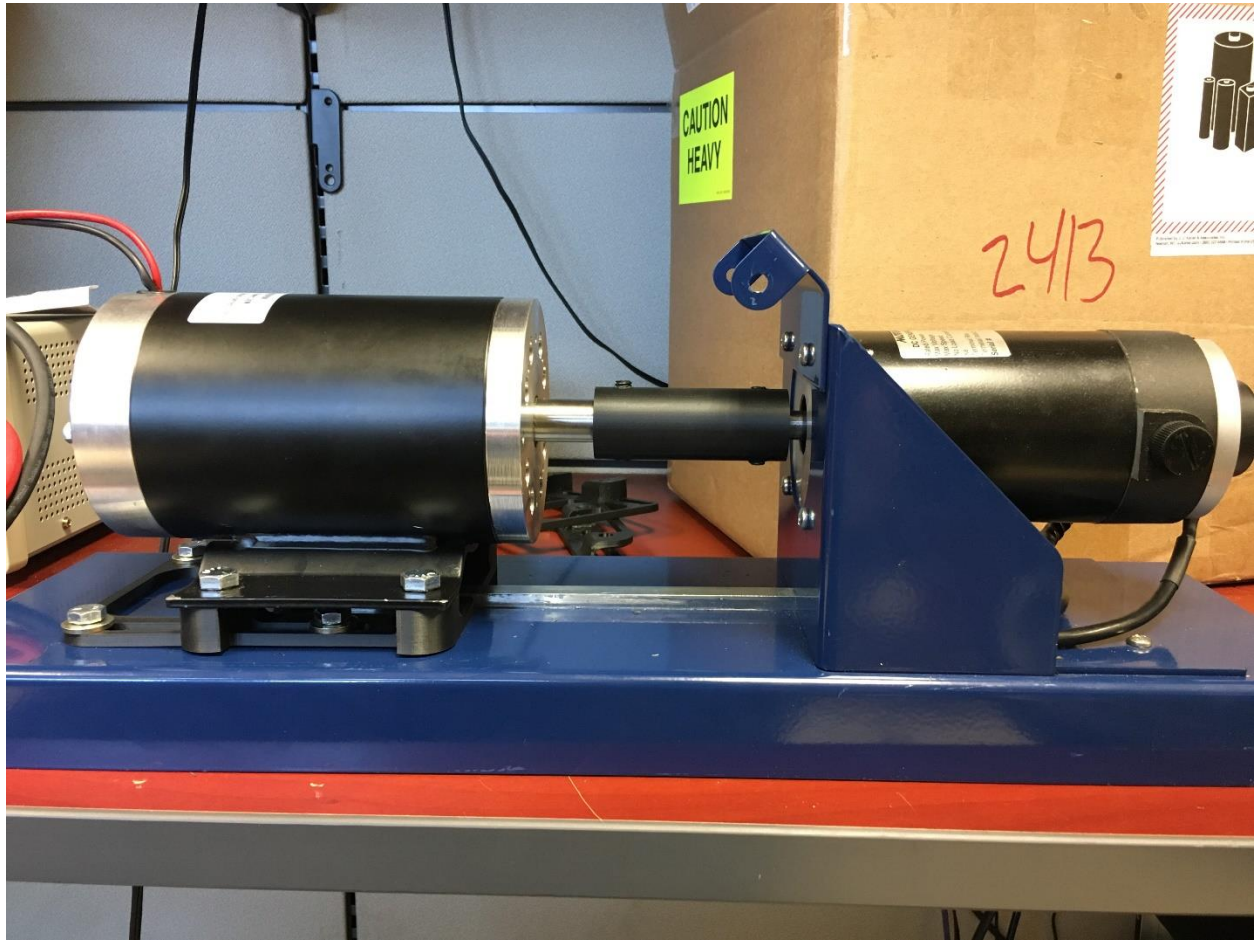


Figure 31 Shanbo EM Motor Coupled to the Motorsolver Generator

Table 18 Encoder Frequency Output and Motor Current Draw

	1 st Generation Motor (FRACMO 624-65-112)	2 nd Generation Motor (Motion Technologies DCA5N242024DL000)	3 rd Generation Motor (Shanbo EM 105ZDY08)
Frequency (kHz)	36.5	33.6	40.0
Current (A)	2.50	2.18	2.27

With the frequency output generated by each motor known, the speed in RPM was calculated in accordance with Equation 12.

$$RPM = f * \frac{60 \frac{s}{min}}{1000 PPR} \quad (12)$$

Table 19 Motor Speed Under Open Circuit Generator Load

	1 st Generation Motor (FRACMO 624-65-112)	2 nd Generation Motor (Motion Technologies DCA5N242024DL000)	3 rd Generation Motor (Shanbo EM 105ZDY08)
Motor RPM	2190	2016	2400
Current (A)	2.50	2.18	2.27

It should be noted that these speeds, though under no intentional load, are subject to the mechanical losses associated with turning the generator. It was therefore necessary to account for these losses and extrapolate to the true no-load speed of the motors. To do this, two ordered pairs were constructed for each motor, one at the speeds and currents in Table 19 above and a second set at full load, zero speed, and full torque. Calculation of the full load current was achieved via Ohm's law, rated motor voltage and the resistance found at the beginning of this chapter.

Table 20 Stall Current of Each Motor

	1 st Generation Motor (FRACMO 624-65-112)	2 nd Generation Motor (Motion Technologies DCA5N242024DL000)	3 rd Generation Motor (Shanbo EM 105ZDY08)
Stall Current (A)	90.9	123.8	155.5

Taking this data and converting them to ordered pairs:

Table 21 Ordered Pairs of Current and Speed

	1 st Generation Motor (FRACMO 624-65-112)	2 nd Generation Motor (Motion Technologies DCA5N242024DL000)	3 rd Generation Motor (Shanbo EM 105ZDY08)
Full Speed (A, RPM)	(2.5, 2190)	(2.18, 2016)	(2.27, 2400)
Full Torque (A, RPM)	(90.9, 0)	(123.8, 0)	(155.5, 0)

Plots of each of these in turn:

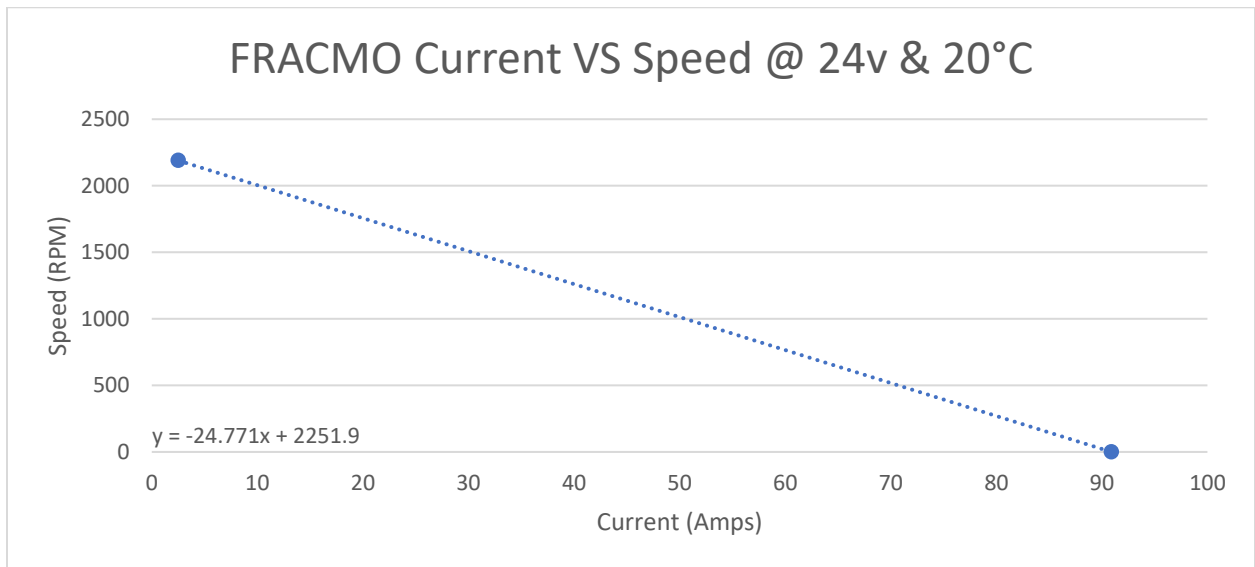


Figure 32 FRACMO Current Versus Speed

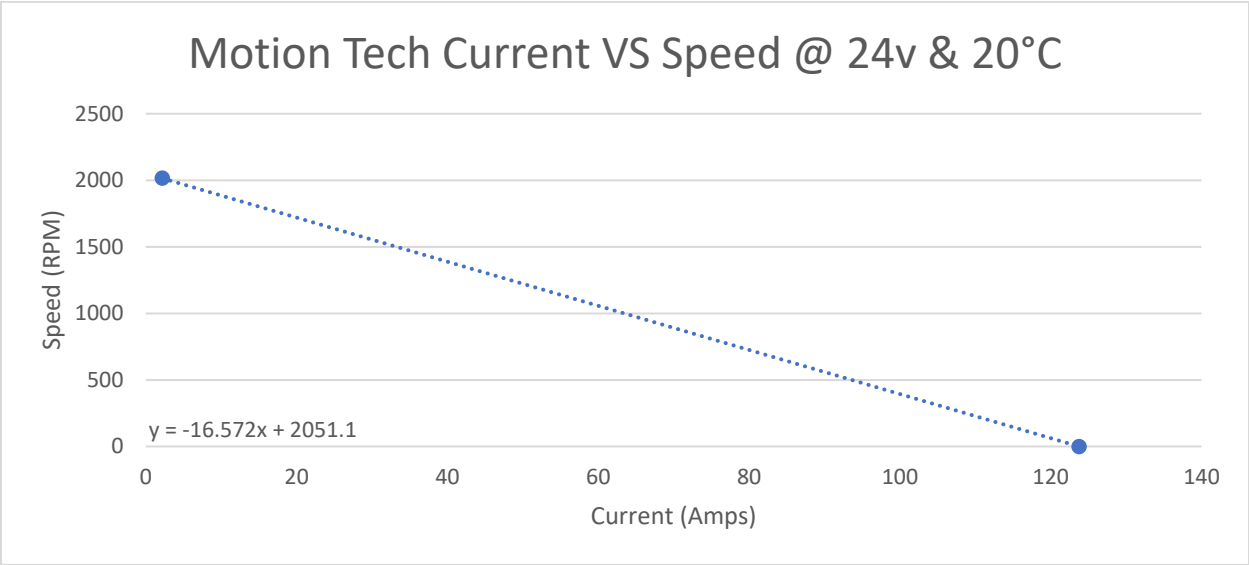


Figure 33 Motion Tech Current Versus Speed

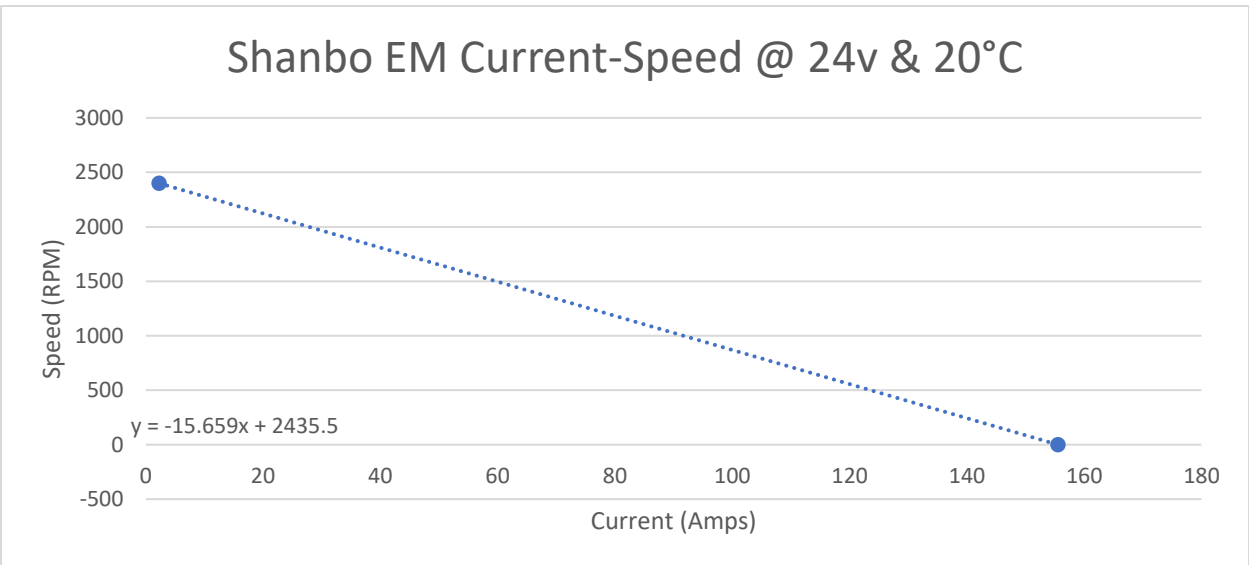


Figure 34 Shanbo EM Current Versus Speed

With the first order polynomial fit, it is possible to read the ideal no load speed from the constant term.

Table 22 Summary of Ideal No-Load Motor Speeds

	1 st Generation Motor (FRACMO 624-65-112)	2 nd Generation Motor (Motion Technologies DCA5N242024DL000)	3 rd Generation Motor (Shanbo EM 105ZDY08)
Ideal No Load Speed (RPM)	2252	2051	2435

The actual no-load speed may then be calculated from the equations listed in figures 33-35 above and the no load currents from each motor. This actual no-load speed comes from the fact that the internal friction and windage take power to overcome and therefore effectively apply a resistance torque to the output shaft.

Table 23 Summary of Actual No-Load Motor Speeds and Currents

	1 st Generation Motor (FRACMO 624-65-112)	2 nd Generation Motor (Motion Technologies DCA5N242024DL000)	3 rd Generation Motor (Shanbo EM 105ZDY08)
Actual No-Load Speed (RPM)	2211	2026	2412
Current (A)	1.65	1.51	1.44

The final step in obtaining the torque speed curves for each of the motors is calculating the torque constant of the motors. With this information, the Current-Speed plots previously generated may be converted to Torque-Speed. When expressed in SI units, the torque constant is simply the inverse of the speed constant. The speed constants were calculated for each motor using Equation 13.

$$K_e = N * \frac{\pi}{30*24} \quad (13)$$

Where K_e is the speed constant in radians per volt-second and N is the actual no load speed of the motor in RPM. The terms $\frac{\pi}{30}$ and $\frac{1}{24}$ come from the conversion of RPM to radians per second

and the rated voltage of the motors, respectively. Applying this equation to each of the no load speeds in the previous table results in the following speed constants:

Table 24 Motor Speed Constants

	1 st Generation Motor (FRACMO 624-65-112)	2 nd Generation Motor (Motion Technologies DCA5N242024DL000)	3 rd Generation Motor (Shanbo EM 105ZDY08)
$K_e \left(\frac{rad}{Vs} \right)$	9.647	8.840	10.524

Taking the reciprocal of each of these constants to obtain the torque constants:

Table 25 Motor Torque Constants

	1 st Generation Motor (FRACMO 624-65-112)	2 nd Generation Motor (Motion Technologies DCA5N242024DL000)	3 rd Generation Motor (Shanbo EM 105ZDY08)
$K_t \left(\frac{Nm}{A} \right)$	0.104	0.113	0.095

Multiplication of these K_t values with the two current values, at no load and full load, from the Current-Speed plots gives the desired Torque-Speed Plots in Figures 36-38 below.

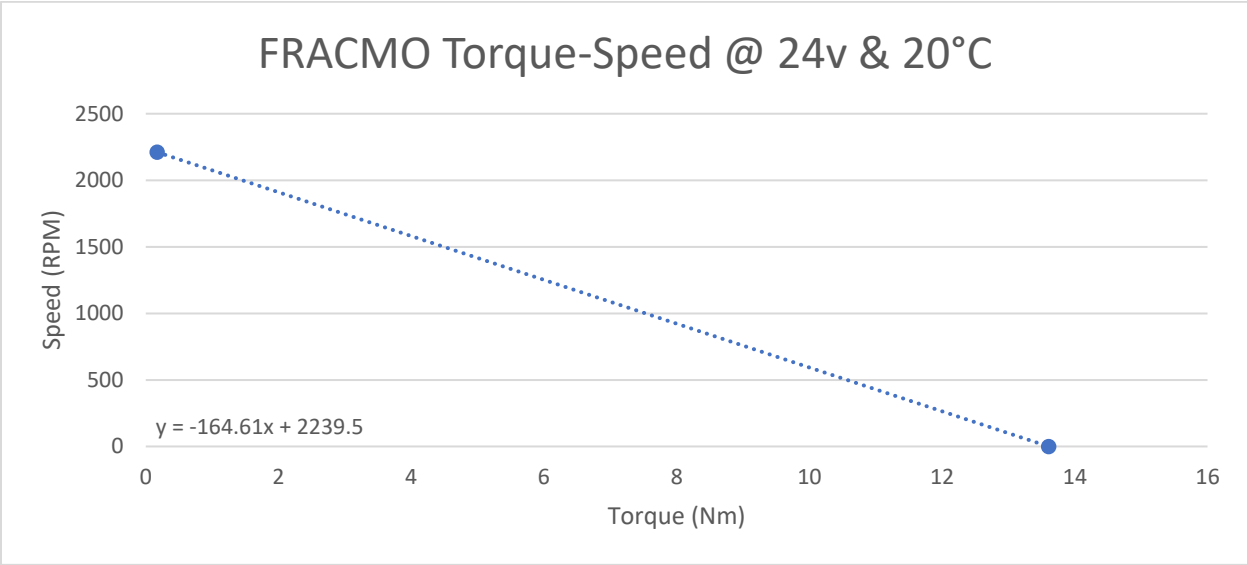


Figure 35 FRACMO Torque-Speed Curve

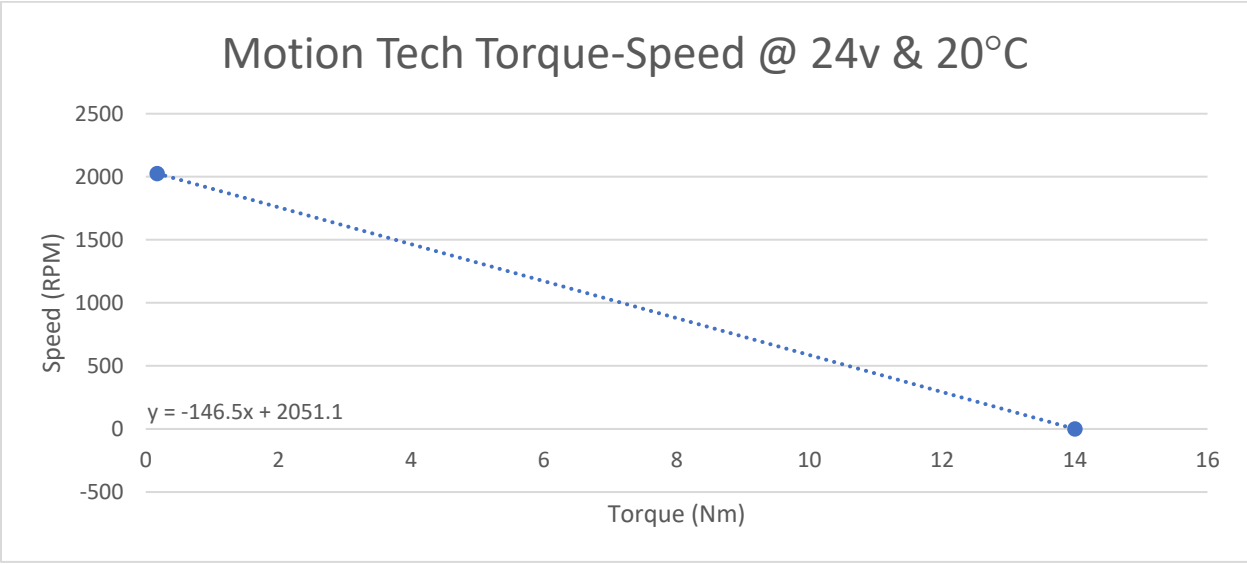


Figure 36 Motion Tech Torque-Speed Curve

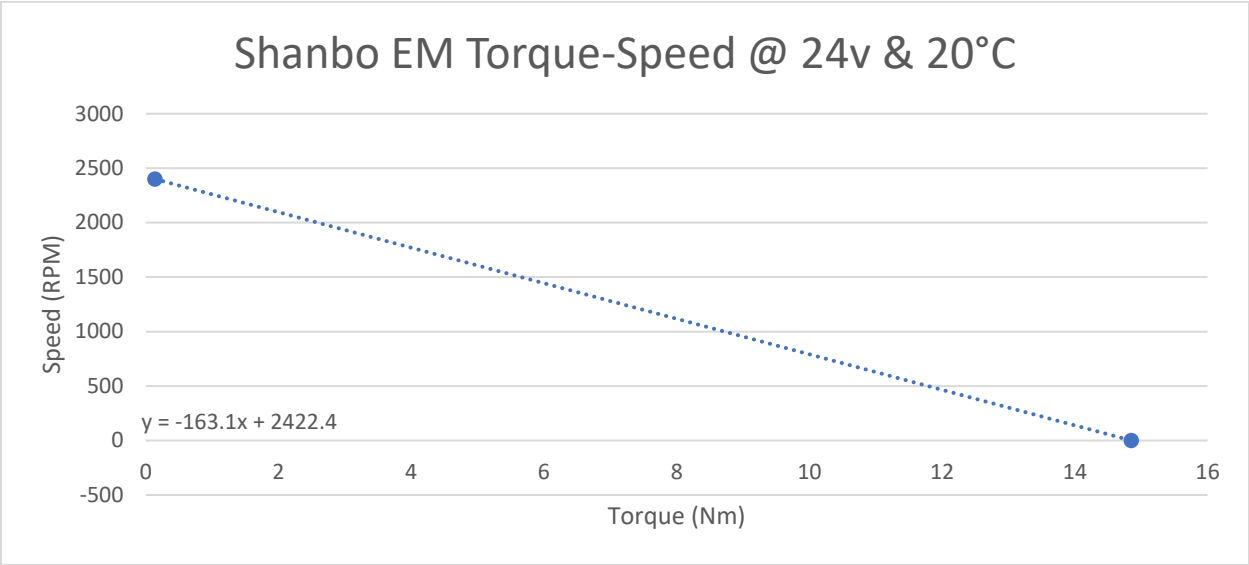


Figure 37 Shanbo EM Torque-Speed Curve

Motor speed regulation, the slope of the torque speed curve, is summarized in the table below for each of the motors:

Table 26 Summary of Motor Regulation

Motor Speed Regulation at 20°C			
	1 st Generation Motor (FRACMO 624-65-112)	2 nd Generation Motor (Motion Technologies DCA5N242024DL000)	3 rd Generation Motor (Shanbo EM 105ZDY08)
Speed Regulation (RPM/Nm)	164.61	146.50	163.10

This metric is useful in determining how much the motor will decrease in speed for a given torque applied to the output shaft.

4.7 Steady State Motor Temperature

The motors used in Greenpower competition are rated at an S1, or continuous, duty cycle. This means they will reach a thermal equilibrium without overheating at most common ambient temperatures. To test where this equilibrium is, the motor was coupled to the Motorsolver generator via the 3D printed coupling in conjunction with the 3D printed base from the no-load speed tests. It should be noted that this test was only conducted on the 3rd generation Greenpower Motor. With this in place, a Dimension Engineering Sabertooth 2X60 regenerative motor controller was used to control power flow to and from the motor and generator, respectively. The controller's ratings are summarized below in Table 27.

Table 27 Motor Controller Ratings

Type	PWM Switching Frequency (kHz)	Input Voltage Range (V)	Continuous Output Current (A)	Peak Output Current (A)
2-Channel, PWM H-Bridge	24	6-30	60	120

With the first channel of the controller connected to the 3rd generation Greenpower motor and the second output channel connected to the Motorsolver generator, the generator was able to act as a variable load on the motor. Three 100Amp Hall Effect current sensors, DROK B07YWVCBRN, were used to determine the current into the controller, motor and generator while the same two multimeters from previous testing scenarios were used to measure the terminal voltages for the motor and generator. Two K-Type thermocouples were secured to the case and end cap of the motor with copper tape as seen in Figure 38. A third K-Type thermocouple was left in open air away from the motors to obtain an accurate reading of the ambient conditions.

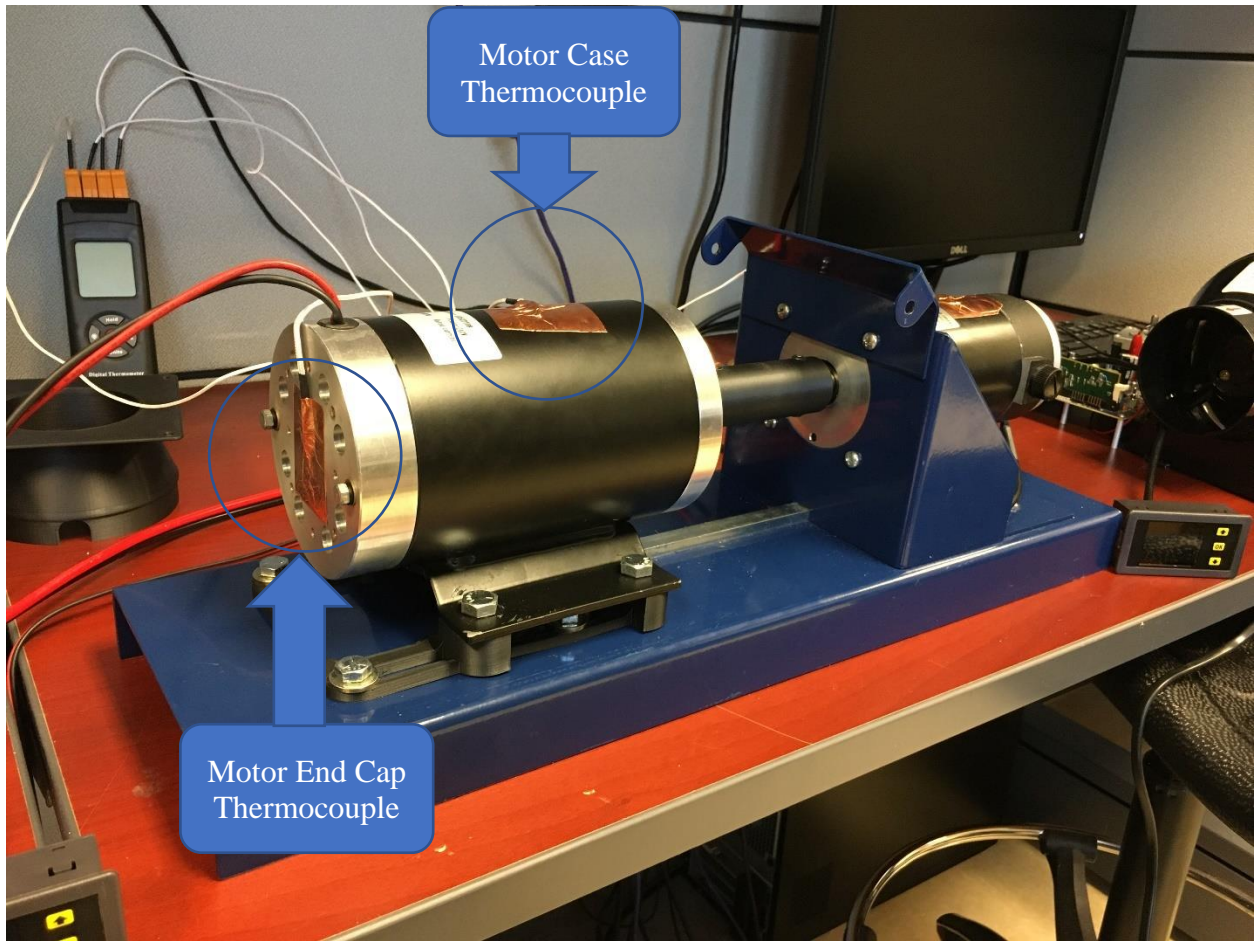


Figure 38 Motor Temperature Setup

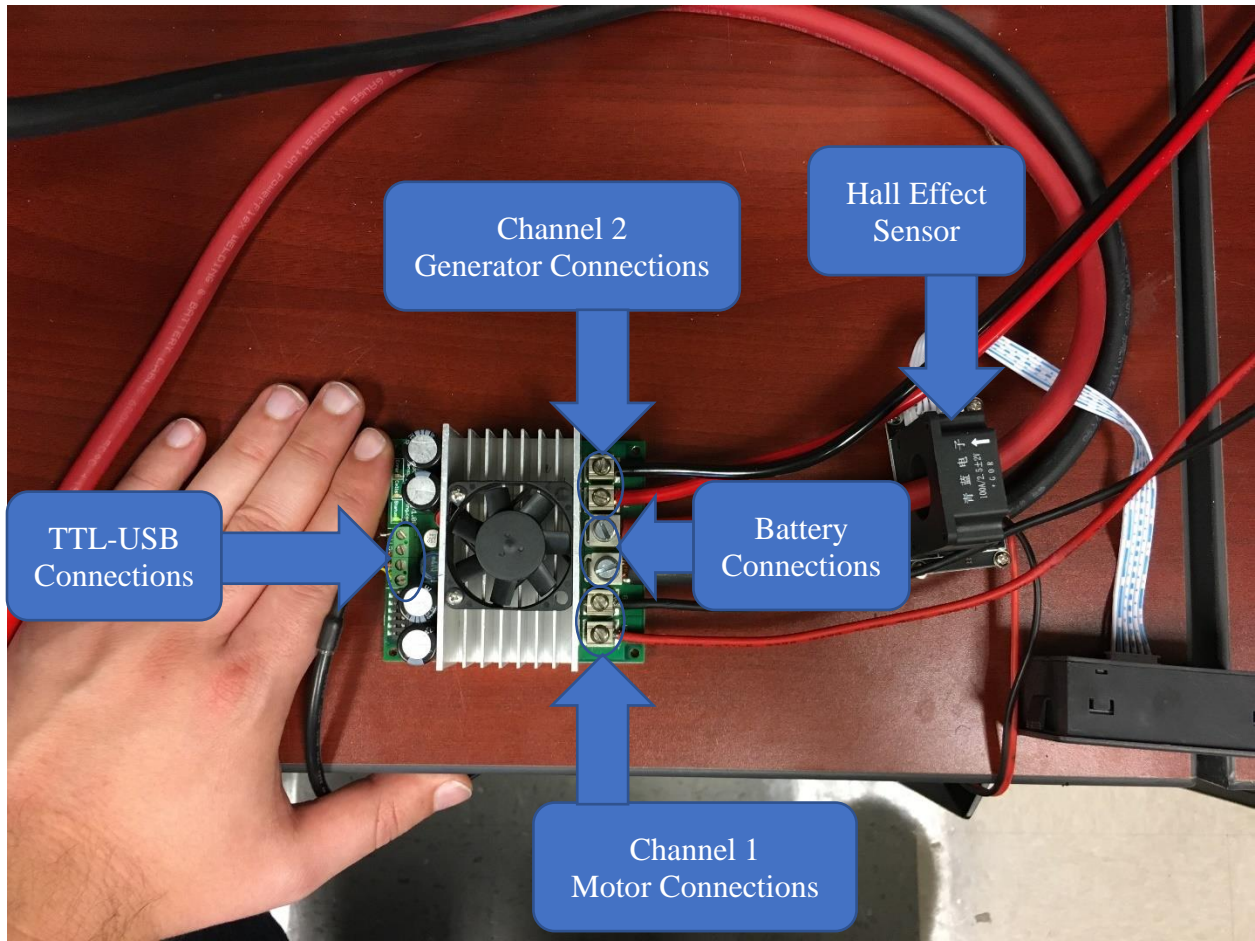


Figure 39 Motor Controller and Connections

With the connections shown above in Figure 39, the software for the motor controller, called DEScribe, was setup in “Custom Test” mode as seen in Figure 40 below. The TTL-USB connections allowed the controller output to be varied from the lab computer.

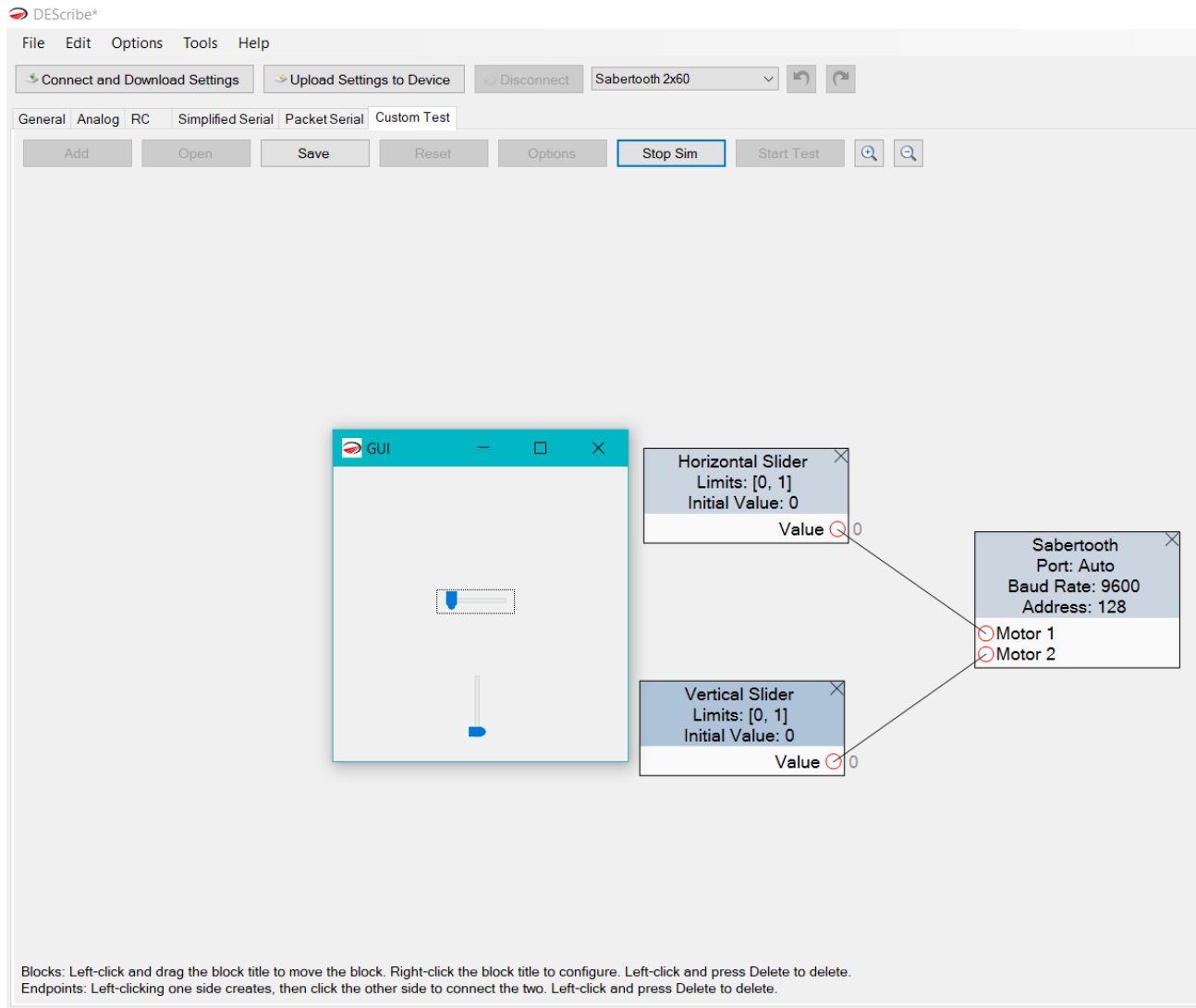


Figure 40 DEDescribe Custom Test Setup

This test setup allowed the input to the motor to be adjusted with the horizontal slider controlling the per-unit motor voltage and the vertical slider controlling the per-unit power voltage of the generator. The test was executed by slowly increasing the motor voltage to its maximum, 24v, value while keeping the generator output as low as possible. In other words, the generator and motor were both operating as motors and rotating at similar speeds in opposite directions such that the generator was helping turn the motor. Once steady full speed was reached on the motor, the voltage applied to the generator was gradually decreased, bringing it back into generator operation, until the rated load of 240W was reached on the motor side input. Then, with the motor controller driving the motor on channel 1 and regenerating on channel 2 for the generator, the power input to the motor was monitored and maintained at 240W for 20-minutes. This test resulted in a temperature rise of 18.6°C, up to 38.6°C from an ambient temperature of 20°C, on the motor. At the 20-minute mark, the 3D printed Carbon Fiber PLA coupler failed as the temperature of the generator shaft became sufficient to distort the bore of the coupler. Despite this failure, when plotting the time versus temperature it can be seen that thermal equilibrium was essentially obtained.

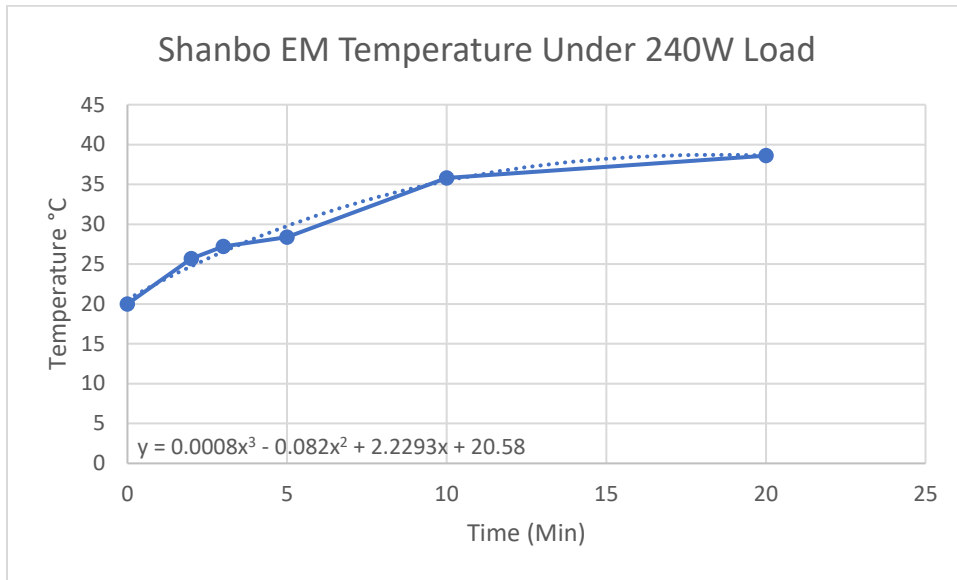


Figure 41 Motor Temperature Versus Time

Observing the slope between each of the datapoints gives a good indication of how fast the temperature of the motor was rising before the failure. Calculation of the slope was achieved by the following formula:

$$Slope \left(\frac{^{\circ}C}{\text{minute}} \right) = \frac{T_2 - T_1}{t_2 - t_1} \tag{14}$$

Where T_1 and T_2 are the initial and final temperatures being considered and t_1 and t_2 are the initial and final times being considered. Performing this calculation for each pair of datapoints yields the following:

Table 28 Motor Temperature Change Per Unit Time

Time Period (minute)	Temperature Change (°C)	Slope (°C/minute)
0-2	20-25.2	2.85
2-3	25.2-27.2	1.5
3-5	27.2-28.4	0.6
5-10	28.4-35.8	1.48
10-20	35.8-38.6	0.28

It can be seen from Table 28 that there is a sharp decrease in slope for the final half of the test. This reduction in slope by an order of magnitude from the initial slope supports that thermal equilibrium was very close to being obtained for the ambient conditions.

CHAPTER V

CONCLUSION AND FUTURE WORK

5.1 Conclusion

This thesis has presented the development of a menu-driven graphical user interface with the objective of supporting students and mentors competing or considering competing in Greenpower Formula 24 events. The modeling underlying the program's functionality has been detailed. The GUI provides a consistent method of introducing concepts involved in motorsports to STEM students and allows them and their mentors to manipulate design variables and observe the effect on performance indicators. Users can access help in the form of descriptive text by pushing a '?' button next to an entity in the GUI. Chapter 1 of this work introduced the background, highlighted of the current void in available software tools to the Greenpower teams and stated the objectives of this work. Chapter 2 reviewed the current state of Formula 24 competition in the US and discussed the differences and similarities between the different classifications as well as more precisely defined the problem being addressed. Chapter 3 provided an overview of the features of the GUI and the processes of developing them. The modeling of the tires, motors, transmission, motor control, batteries and aerodynamics were all discussed. The development of the models varied in complexity, but all had the common objective of covering the major variables. The method by which forces, and power effected the car in the program were also explored. Output Plots and Help functions were other features of

the interface examined in this chapter. Experimental tests conducted to support the development of the models used in the interface were discussed in Chapter 4. Testing of the actual hardware used in competition provided an element of practical application otherwise missing in this context. Chapter 4 may also serve as a guide to those recreating the test conditions for their specific machines and as a reference for testing future generations of hardware. This thesis has developed a powerful tool which will allow mentors to engage their students more thoroughly and consistently in STEM activities. Whether it be in an experiment, simulation or during a race, students and mentors alike will gain a fundamentally better understanding of their vehicles from the use of this application.

5.2 Future Work

There are several opportunities to expand on the present work. For example, additional design optimization studies can be added including gear ratio and motor control. To explore higher modeling accuracy and higher efficiency targets may be possible by including skin effects, hysteresis and switching losses. A more accurate representation of the terrain, for example to model inclines, would improve calculations of the output values from the GUI. The continuation of this work in the future will provide the opportunity to validate the models used in this application. Advanced concepts such as optimization techniques and investigation of alternative motor technologies can be introduced specifically for the college level participants (not currently included in US competitions). Performance comparison with alternative green motor technologies such as switched reluctance motors, which are gaining popularity in use with electric vehicles, can be used to enhance knowledge of green energy and sustainability concepts.

Finally, to broaden the educational impact of the GUI, it can be incorporated into pre-packaged and ready to use project-based learning modules that teachers can use in their classrooms including teachers who are not competing in the race or who lack support to build their own modules.

REFERENCES

- [1] A. D. L. H. B.-d. P. J. & V. P. P. Struyf, "Students' engagement in different STEM learning environments: integrated STEM education as promising practice?," *International Journal of Science Education*, vol. 41, no. 10, pp. 1387-1407, 2019.
- [2] P. Hylton, "Using Motorsports Design Concepts to Further STEM Education," *The Journal of Technology Studies*, vol. 36, no. 1, pp. 12-15, 2010.
- [3] D. J. R. Pete Hylton, "Motorsports Engineering: Bridging the Divide between Engineering and Engineering Technology with an Industry-Focused Curriculum," *Journal of Engineering Technology*, vol. 31, no. 2, p. 32, 2014.
- [4] E. R. George J Delagrammatikas, "Board 113: Teaching Hands-On Racecar Design in a Summer Pre-College," in *ASEE 2019 Annual Conference*, 2019.
- [5] "EERE Success Story—Utah Launched Greenpower Electric Car Challenge to Engage Students in STEM," 7 9 2018. [Online]. Available: <https://www.energy.gov/eere/success-stories/articles/eere-success-story-utah-launched-greenpower-electric-car-challenge>. [Accessed 21 7 2021].
- [6] G. U. Foundation, 2021. [Online]. Available: <https://greenpowerusa.net/f24-grades-6-12>. [Accessed 12 7 2021].
- [7] G. U. Foundation, "F24 Rules and Regulations 2020-2021 Race Season," 2021. [Online]. Available: https://drive.google.com/file/d/1ZhlwFRU6hy7dt62gaH8lzn3Eq_lmGHDT/view. [Accessed 12 7 2021].
- [8] EPA, "Fuel Economy," 2021. [Online]. Available: <https://fueleconomy.gov/feg/PowerSearch.do?action=noform&path=1&year1=1984&year2=2021&vtype=Electric&pageno=1&rowLimit=50>. [Accessed 12 7 2021].
- [9] EPA, "Alternative Fuels Data Center," 2021. [Online]. Available: <https://afdc.energy.gov/data/>. [Accessed 12 7 2021].
- [10] J. Bireman, "Tubeless vs Latex Tube vs Butyl, Rolling Resistance Compared," 2014. [Online]. Available: <https://www.bicyclerollingresistance.com/specials/tubeless-latex-butyl-tubes>. [Accessed 12 7 2021].
- [11] J. Bireman, "Road Bike Tire Test: Schwalbe Durano," 2015. [Online]. Available: <https://www.bicyclerollingresistance.com/road-bike-reviews/schwalbe-durano-2015>. [Accessed 12 7 2021].
- [12] J. Bireman, "Touring Bike Tire Test: Schwalbe Kojak," 2017. [Online]. Available: <https://www.bicyclerollingresistance.com/tour-reviews/schwalbe-kojak-2017>. [Accessed 12 7 2021].

- [13] O. W. S. S. a. S. P. Paul Krause, "DC Machines and Drives," in *Analysis of Electric Machinery and Drive Systems*, John Wiley & Sons, Inc, 2013, p. 377.
- [14] "Motor Performance Graphs," [Online]. Available: <http://www.greenpower.beamweb.co.uk/files/TechnicalInfo/GreenpowerF24PerformanceGraph.pdf>. [Accessed 12 7 2021].
- [15] 4QD, "Greenpower," [Online]. Available: <https://www.4qd.co.uk/docs/greenpower/>. [Accessed 12 7 2021].
- [16] D. Montone, "Temperature Effects on Motor Performance," 2014. [Online]. Available: https://www.haydonkerkpitman.com/-/media/ametekhaydonkerk/downloads/white-papers/temperature_effects_on_dc_motor_performance_1.pdf?la=en. [Accessed 12 7 2021].
- [17] S. C. Burgess, "Improving cycling performance with large sprockets," *2nd International Conference on the Engineering of Sport*, pp. 23-29, 1998.
- [18] F. V. J. V. M. J. M. W. V. A. Peter Van den Bossche, "SUBAT: An assessment of sustainable battery technology," *Journal of Power Sources*, p. 914, 2006.
- [19] W. H. M.E. Glavin, "Optimisation of a photovoltaic battery ultracapacitor hybrid energy storage system," *Solar Energy*, vol. 86, no. 10, pp. 3009-30020, 2012.
- [20] Yuasa Batteries, "Yuasa REC Batteries," [Online]. Available: <https://www.yuasabatteries.co.nz/content/documents/deep-cycle/yu109-2100-yuasa-rec36-12-final.pdf>. [Accessed 12 7 2021].
- [21] AJC Battery, "Sealed Lead Acid Batteries AJC-D35S," [Online]. Available: <https://cdn.shopify.com/s/files/1/2867/7354/files/BatteryClerk-AJC-Battery-D35S.pdf?8876048441346863915>. [Accessed 12 7 2021].
- [22] S. C. J. S. M. a. M. J. Lee, "Modeling and Validation of 12V Lead-Acid Battery for Stop-Start Technology," *SAE International*, 2017.
- [23] SimScale, "Tutorial: Aerodynamics Simulation of Flow Around a Vehicle," 18 6 2021. [Online]. Available: <https://www.simscale.com/docs/tutorials/aerodynamic-simulation-vehicle/>. [Accessed 12 7 2021].
- [24] Tektronix, "Capacitance and Inductance Measurements Using an Oscilloscope and a Function Generator," [Online]. Available: <https://www.tek.com/document/application-note/capacitance-and-inductance-measurements-using-oscilloscope-and-function-ge>. [Accessed 12 7 2021].
- [25] National Institute of Technology, "Testing of DC Machines," [Online]. Available: <http://nit-edu.org/wp-content/uploads/2019/06/ch-31-Testing-of-dc-machines.pdf>. [Accessed 12 7 2021].
- [26] T. Barnaby, 29 9 2013. [Online]. Available: Green Sim – Greenpower Car Simulator. [Accessed 12 7 2021].
- [27] A. A. M. B. J. C. K. G. W. G. Sertac Karaman, "Project-based, Collaborative, Algorithmic Robotics for High School Students: Programming Self-driving Race Cars at MIT," in *IEEE Integrated STEM Conference*, 2017.

VITA

Andrew Rivers, born July 7, 1991, in Fort Wayne Indiana, received his B.S. in Electrical Engineering from the University of Memphis in 2014. At the University of Memphis, he was a member of the university's SAE Baja car team as a driver and oversaw the electrical systems of the car. He worked at Ring Container programming production line PLC's and then at Olympus Surgical Technologies as a Sustaining Engineer after his graduation. He moved to Chattanooga to pursue his master's in electrical engineering in late 2018 and has recently accepted a position with Zero Motorcycles as a Test Engineer in Research and Development in Scotts Valley California.